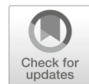

Stress Evolution and Cracking in Sol-Gel-Derived Thin Films

11

Hiromitsu Kozuka

Contents

Introduction 276
Stress Evolution in Gel Films during Heating 277
  Origins of the Stress Evolution 277
  Measurement of Intrinsic Stress 278
  Effect of the Amount of Water for Hydrolysis 280
  Effect of Chelating Agents 282
  Effect of Methyltriethoxysilane 284
  Effect of PVP 286
Crack Formation in Gel-Derived Coatings 287
  Macroscopic Cracking versus Microscopic Cracking 287
  In Situ Observation of Cracking 288
  Macroscopic Crack Formation in the Heating-Up Stage 289
  Effect of Thickness 290
  Effect of Heating Rate 290
  Effect of the Amount of Water for Hydrolysis 291
  Effect of Humidity 293
Strategy for Thick Film Formation without Macroscopic Cracking 294
  Thick Film Formation via Non-cycled Deposition in Literature 294
  Polyvinylpyrrolidone for Thick Film Formation 295
Residual Stress of Gel-Derived Coatings 299
Concluding Remarks 307
References 308

H. Kozuka (✉)
Department of Chemistry and Materials Engineering, Faculty of Chemistry, Materials and Bioengineering, Kansai University, Osaka, Japan
e-mail: kozuka@kansai-u.ac.jp

© Springer International Publishing AG, part of Springer Nature 2018

L. Klein et al. (eds.), *Handbook of Sol-Gel Science and Technology*,
https://doi.org/10.1007/978-3-319-32101-1_12

Abstract

The author's group has studied the stress evolution and cracking in gel films during heating, the strategy for preparing thicker, crack-free films, and the effect of heat-treatment temperature on residual stress of gel-derived ceramic thin films. In this chapter, what the author's group has clarified on these issues is described, where related literature is also reviewed.

Gel films acquire in-plane tensile stress during heating, which is affected by various processing parameters including the water-to-alkoxide ratio, the additives like chelating agents and organic polymers, and heating rate. In situ observation of gel films under heating indicated that macroscopic cracking occurs in the heating-up stage and that the cracking onset temperature is affected by heating rate, film thickness, water-to-alkoxide ratio, and humidity. The strategy for thick film formation without cracking via non-cycled deposition is reviewed, and the addition of polyvinylpyrrolidone is demonstrated to be effective in increasing the uncracking critical thickness.

The in-plane residual stress was measured on YSZ films that were deposited on silicon substrates and fired at various temperatures. The dependence of the residual stress on the firing temperature was rather complex, but could be understood in terms of the increase in intrinsic stress during heating due to densification, the structural relaxation at low and high temperatures, and the thermal stress that is generated during cooling.

Introduction

Sol-gel technique for depositing ceramic thin films has already had long history. It has attracted many people because the whole process can be conducted under the ambient pressure. The most scientific issues on sol-gel processing are very widely and deeply discussed and documented in the great book, *Sol-gel Science: The Physics and Chemistry of Sol-gel Processing* authored by Brinker and Scherer, which was published in 1990 (Brinker and Scherer 1990). Although more than a quarter of a century has passed, nobody thinks that this book is out-of-date, and every scientist comes back to it when encountering scientific problems. As far as sol-gel coating is concerned, how the processing parameters affect the thickness, structure, and porosity is precisely discussed in the book, which offers us the most important understanding of the scientific aspects of sol-gel thin film deposition.

However, there are still scientific issues left to be studied so that the sol-gel technique is utilized for thin film production, especially in industrial scale. The issues on crack formation and stress evolution are the examples. When gel films are fired to be converted into ceramic films, in-plane stress is generated, which leads to crack formation (Hu et al. 1988; Atkinson and Guppy 1991; Scherer 1992; Brinker et al. 1992). Such cracking occurs especially when the original gel films are large in thickness. The uncracking critical thickness, which is the maximum thickness achievable on single-step deposition and firing without cracking, is less than

100 nm for sol-gel-derived oxide thin films (ca 500 nm for silica films). On the other hand, thin film devices often need thickness over submicron so that they have desired performances. Then, in order to achieve thickness over submicron without cracking, the gel film deposition and firing should be cycled, which, however, is troublesome in production. The first thing that should be done is to clarify how the processing parameters affect the stress evolution on gel-to-ceramic film conversion.

The residual stress is the stress that is measured at room temperature after the whole deposition process. Such residual stress affects the properties and performance of thin film devices (Rossetti et al. 1991; Desu 1994; Lee et al. 1994; Sengupta et al. 1998; Gupta 2002; Yao et al. 2003; Lian and Sottos 2004; Zhang et al. 2004; Ohno et al. 2006; Corkovic et al. 2008; Ohno et al. 2008). The degree of the substrate bending is also a function of the residual stress (Lu et al. 2006). Therefore, how to control the residual stress is important from the viewpoint of technological use of thin films. In order to know how to control the residual stress, the effects of the processing parameters on the residual stress should be clarified.

The author's group has been studying the issues on the stress evolution and cracking as well as the strategy for preparing thicker, crack-free films and on the residual stress for sol-gel-derived oxide thin films. In this chapter, what the author's group has clarified on these issues is described.

Stress Evolution in Gel Films during Heating

Origins of the Stress Evolution

Gel films undergo changes in structure and chemistry when heated, which results in evolution of stress. The stress that is of concern here is the so-called intrinsic stress, which is defined as the stress measured in situ at any moment of film formation, and is distinguished from "residual stress," which is measured at room temperature after film formation. When heated, for instance, up to 500 °C, gel films are densified accompanied with several tens % reduction in volume due to (a) capillary pressure on solvent vaporization and (b) condensation reaction. Densification leads to the evolution of in-plane tensile stress because the films are constrained on the substrates. The strain in the film due to such densification is of the order of 10^{-1}, while the strain that the substrate may have due to its thermal expansion would be of the order of 10^{-3} to 10^{-2} when the film on the substrate is heated up to 500 °C, for instance. Therefore, the stress due to densification would be dominating in the heating-up stage for gel films. When the films are heated over 500 °C, where many of the oxide thin films are crystallized, the stress relaxation would occur due to accelerated atomic diffusion, which will be described in section "Residual Stress of Gel-Derived Coatings."

In the cooling-down stage, on the other hand, no major changes are expected in structure and chemistry. Therefore, it would be the thermal stress that is generated in the cooling-down stage, i.e., the stress due to the difference in thermal expansion

coefficient between the film and the substrate. The final stress that is measured at room temperature is the "residual stress."

Several papers have been published so far on the measurement of stress in gel-derived films as summarized in Table 1. Stress evolution occurring on gel film firing is well documented as is seen in the table. Particularly, tensile stress evolution accompanied by polycondensation reaction in the heating-up stage was clearly demonstrated on TEOS-derived silica gel films by Parrill, who made in situ measurement of stress by measuring the substrate curvature by laser beam and also measured infrared (IR) absorption spectra of the films (Parrill 1994). Such stress generated in the heating-up stage causes macroscopic cracking or delamination as will be described in section "Crack Formation in Gel-Derived Coatings."

Densification of gel films occurring on firing is greatly affected by sol-gel chemistry. From the viewpoint of technological aspects of sol-gel deposition of ceramic thin films, knowledge on the practical effects of the processing parameters on stress evolution is important, for example, the conditions for hydrolyzing alkoxides, the substrate withdrawal and rotation speed, the heat-treatment conditions, etc. In the following sections, intrinsic stress measured on heating is described on gel films prepared under different conditions.

Measurement of Intrinsic Stress

In-plane stress can be obtained for a film deposited on one side of a substrate by measuring the curvature of the substrate bending. In-plane stress of the film, σ, is calculated using Stoney's equation (Hoffman 1966):

$$\sigma = \frac{1}{6}\frac{E_s}{1-\nu_s}\frac{{t_s}^2}{t_f}\frac{1}{\Delta R} \quad (1)$$

where $E_s/(1-\nu_s)$ is the biaxial elastic modulus of the substrate; t_s and t_f are the thickness of the substrate and film, respectively; and ΔR is defined by the following equation:

$$\Delta R = \frac{R_1 R_2}{R_1 - R_2} \quad (2)$$

where R_1 and R_2 are the radii of the curvature of the bare and coated substrates, respectively. When R_2 and t_f are measured as a function of temperature during heating, we may obtain the variation of intrinsic stress during heating. (In the strict sense, t_s, $E_s/(1-\nu_s)$, and R_1 should be measured at the temperature of interest as well as R_2 and t_f. However, t_s, $E_s/(1-\nu_s)$, and R_1 can be assumed to be constant during heating to a good approximation, and those measured at room temperature can be used for calculating σ.)

In the experimental work described in the following sections, the gel films were deposited on single-crystal Si wafers and heated at a constant rate of 5 °C min^{-1} up to 500 °C. The measurement was conducted using an apparatus equipped with a

Table 1 Stress measurement on gel-derived coatings in literature (not including ours)

Film	Stress measurement	Remarks	References
PZT	Substrate deflection	Stress-induced deflection models	Pulskamp et al. (2003)
$SrBi_2Ta_2O_9$	X-ray diffraction	Effects of heating atmosphere on residual stress	Hartner et al. (2003)
TEOS-GPTMS	Substrate deflection	Effects of curing temperature on residual stress	Robertson et al. (2003)
PZT	Substrate deflection	Effects of Pt/Ti underlayers on residual stress	Zhang et al. (2002)
$BaTiO_3$	Raman spectroscopy and X-ray diffraction	Effect of thickness	Gupta (2002)
ZrO_2	Substrate deflection	Effect of viscous flow, acetate ions, and moisture	Brenier and Gagnaire (2001), Brenier (2002)
SiO_2	Substrate deflection	Stress evolution during heating up, annealing, and cooling down	Chiang et al. (2000)
SiO_2	Substrate deflection	Determination of biaxial modulus and linear thermal expansion coefficient of films	Chow et al. (2000)
ZrO_2	Substrate deflection	Stress evolution during polycondensation and acetylacetone elimination	Brenier et al. (1999)
$PbTiO_3$	Substrate deflection	Stress evolution during heating. Effect of solvent/polymeric network interaction, thermal expansion mismatch, and crystallization	Sengupta et al. (1998)
(Pb,Ca) TiO_3	Substrate deflection	Stress evolution during drying, thermal treatment, and crystallization	Mendiola et al. (1998)
ZrO_2	X-ray diffraction	Residual stress correlated with phase transformation	Mehner et al. (1997)
PZT	Substrate deflection	Residual stress	Tuchiya et al. (1996)
$PbTiO_3$	Raman spectroscopy	Dependence on position	Chingprado et al. (1995)
SiO_2	Substrate deflection	Stress evolution during heating	Parrill (1994)
TiO_2-doped SiO_2	Substrate deflection	Stress evolution during heating	Syms and Holmes (1994a)
$YBa_2Cu_3O_x$	Shadow moiré interferometry	Residual stress. Dependence on position	Wu et al. (1993)
TiO_2	Real-time Raman spectroscopy	Effect of crystallization and deposition temperature	Exarhos and Hess (1992)
SiO_2, TiO_2	Modulated transmission ellipsometry	Residual stress. Effect of drying and heating conditions	Cerqua et al. (1988)
PZT	Substrate deflection	Residual stress. Effect of crystalline phases and their orientation	Corkovic et al. (2008)

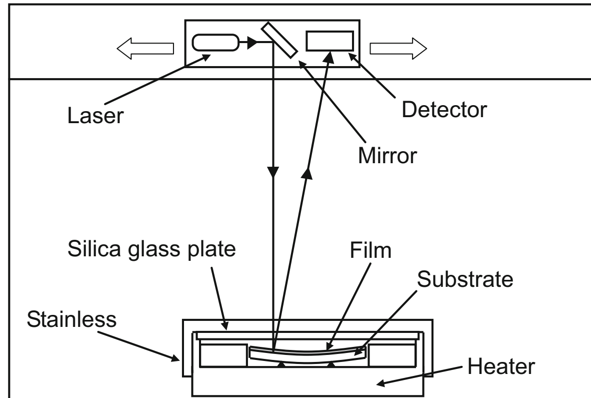

Fig. 1 Apparatus for in situ stress measurement in films during heating (Model FLX-2320, KLA-Tencor, San Jose, USA)

heater, where the radius of the curvature of the substrate surface was monitored by laser beam (Fig. 1). $E_s/(1-\nu_s)$ was assumed to be 1.8505 × 10^{11} and 2.290 × 110^{11} Pa for Si(100) and Si(111) substrates, respectively, and R_1 values measured at room temperature were employed. For measuring t_f, a part of the gel film was scraped off with a surgical knife, and the level difference thus made on the substrate was measured using a contact probe surface profilometer. The films were made thin enough to avoid cracking, and the absence of cracks was examined after each run of in situ stress measurement.

Effect of the Amount of Water for Hydrolysis

A number of processing parameters affect the densification behavior of gel films, which accordingly affects the stress evolution and crack formation in the heating-up stage. The extent of the hydrolysis of alkoxides is one of the factors that could affect the densification behavior and hence the stress evolution in films. In order to know how the amount of water for alkoxide hydrolysis affects the stress evolution, in situ stress measurement was conducted during heating on alkoxide-derived silica gel films deposited on single-crystal Si substrates (Kozuka and Komeda 2004).

Starting solutions of mole ratios, TEOS : H_2O : HNO_3 C_2H_5OH = 1 : x : 0.01 : 4, were prepared where x = 2, 4, and 10. The solutions thus obtained were kept in sealed glass containers at 30 °C for 24 h and served as coating solutions. Spin coating was performed on single-crystal Si(100) substrates at a spinning rate of 500, 900, or 3500 rpm. Immediately after deposition, the gel films were served for in situ stress measurement.

Figure 2 shows the relationship between the thickness and temperature, measured on films that were deposited at 3500 rpm and heated isothermally and successively at intervals of 50 °C up to 500 °C, where 10 min heat treatment was conducted at each temperature. The thickness decreased with temperature, where the proportion of thickness reduction at 500 °C was almost the same at 24–25% irrespective of the

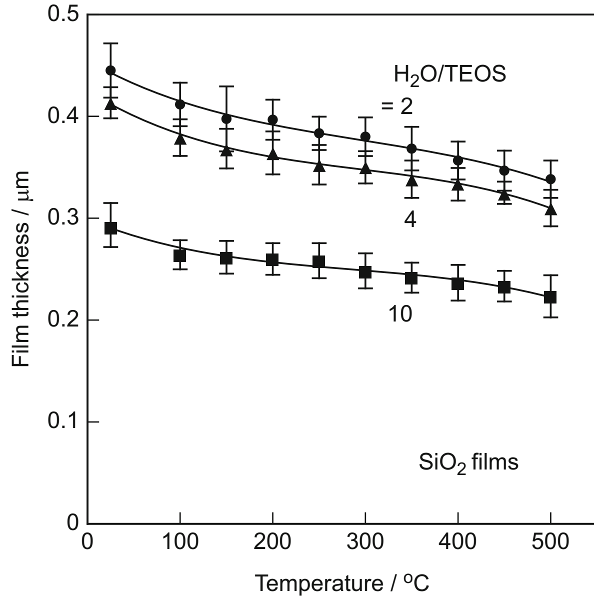

Fig. 2 Reduction in thickness on heat treatment for silica coatings prepared on single-crystal Si substrates from TEOS solutions of different H_2O/TEOS mole ratios (Kozuka and Komeda 2004)

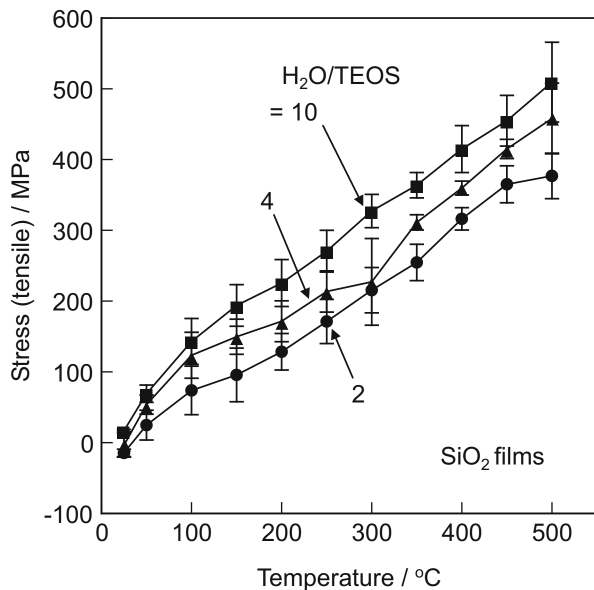

Fig. 3 Variation of in-plane stress as a function of temperature for silica coatings prepared on single-crystal Si substrates from TEOS solutions of different H_2O/TEOS mole ratios (Kozuka and Komeda 2004)

H_2O/TEOS ratio. The stress in films is plotted against temperature in Fig. 3. The stress is tensile, and increases with increasing temperature, which results from densification of films in the course of heating. Higher stress is found when the films are prepared from solutions of higher H_2O/TEOS ratios.

One possible reason for the higher stress at higher H_2O/TEOS ratios is the larger extent of polycondensation reaction occurring in gel films on heating, which is allowed by the larger amount of the OH groups susceptible to polycondensation reaction. However, the slope of the stress–temperature relation is similar irrespective of the H_2O/TEOS ratios at temperatures over 100 °C, where the polycondensation reaction proceeds (Fig. 3) and the proportion of reduction in thickness is similar (Fig. 2), the latter of which implies that there is no evident difference in densification between different H_2O/TEOS ratios. On the other hand, the slope of the stress–temperature plots below 100 °C is larger for H_2O/TEOS = 4 and 10 than for H_2O/TEOS = 2 (Fig. 3). The capillary pressure is proportional to the surface tension of the vaporizing liquid (Brinker and Scherer 1990). Because H_2O has much higher surface tension (72 mN m^{-1}) than C_2H_5OH (22 mN m^{-1}), the capillary pressure would be higher at larger H_2O/TEOS ratios. This would be one of the reasons for the larger slope of the stress–temperature relation observed below 100 °C at higher H_2O/TEOS ratios.

Lower H_2O/TEOS ratios especially at 2 could result in siloxane polymers with less developed network structure. Such structure would promote structural relaxation, leading to smaller rates of increase in stress during heating. However, the slope of the stress–temperature relation was similar over 100 °C irrespective of the H_2O/TEOS ratios. Therefore, the structural relaxation is ruled out as the origin of the lower stress observed at lower H_2O/TEOS ratios. It would be the higher capillary pressure that causes higher stress at higher H_2O/TEOS ratios as discussed above.

Effect of Chelating Agents

Chelating agents are often used to stabilize alkoxides such as titanium and zirconium alkoxides. Chelating agents block the hydrolysis of alkoxides, which could hinder the progress of polycondensation reaction in films as in solutions. Therefore, chelating agents could affect the densification behavior of gel films and hence stress generation during heating. How the chelating agents could affect the stress evolution was examined on titania gel films by in situ stress measurement (Ishikawa and Kozuka 2004; Ishikawa 2004).

Starting solutions of mole ratios, $Ti(OC_3H_7^i)_4 : HNO_3 : H_2O : C_2H_5OH = 1 : 0.2 : 1 : 30$, $Ti(OC_3H_7^i)_4 : X : HNO_3 : H_2O : C_2H_5OH = 1 : 2 : 0.2 : 1 : 30$, were prepared where X is chelating agents, i.e., CH_3COOH and $CH_3COCH_2COCH_3$. A solution with no chelating agents was also prepared, where $Ti(OC_3H_7^i)_4 : HNO_3 : H_2O : C_2H_5OH = 1 : 0.2 : 1 : 30$. The starting solutions were kept in sealed glass containers at room temperature for 24 h and then were served as coating solutions. Spin coating was conducted at a spinning rate of 2000 rpm. Immediately after deposition the gel films were served for in situ stress measurement.

X-ray diffraction measurements indicated that all the films are amorphous below 400 °C while crystallized into anatase between 400 °C and 500 °C. The film prepared without chelating agents showed major reduction in thickness below

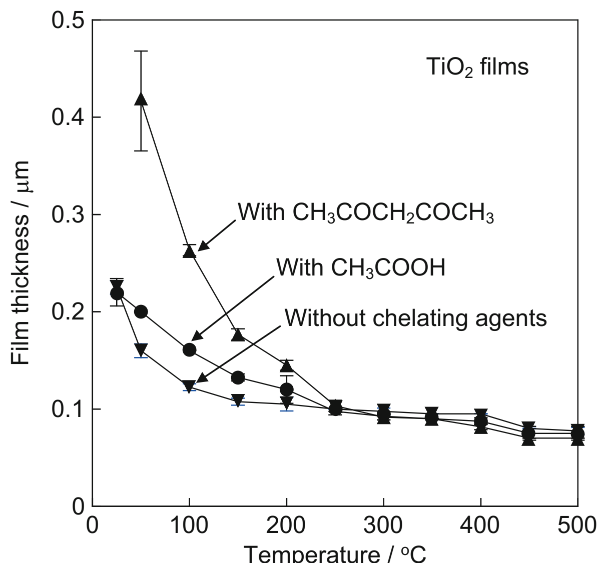

Fig. 4 Reduction in thickness on heat treatment for titania coatings prepared on single-crystal Si substrates from solutions with and without chelating agents (Ishikawa and Kozuka 2004; Ishikawa 2004)

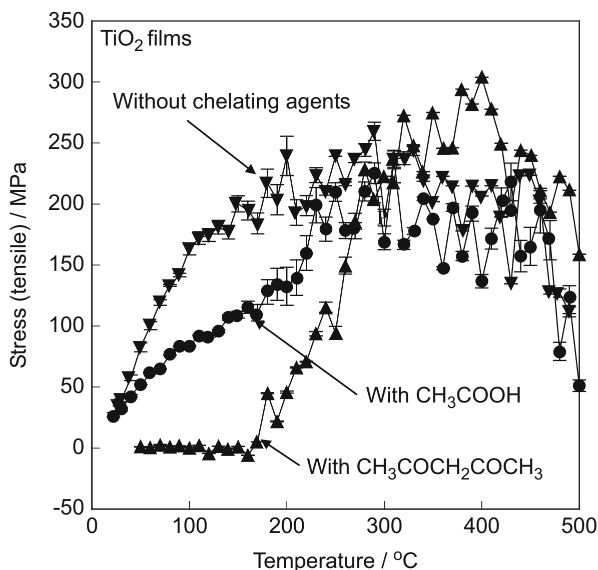

Fig. 5 Variation of in-plane stress as a function of temperature for titania coatings prepared on single-crystal Si substrates from solutions with and without chelating agents (Ishikawa and Kozuka 2004; Ishikawa 2004)

150 °C (Fig. 4), while the stress increased significantly (Fig. 5), suggesting that the stress evolution results from the film densification.

The film prepared with CH_3COOH showed more gradual reduction in thickness below 200 °C (Fig. 4), which resulted in more sluggish increase in stress (Fig. 5). Lower volatility of CH_3COOH than alcohols may have induced such more gradual reduction in thickness. The stress began to increase more steeply at 200 °C (Fig. 5),

where a significant loss of CH_3COO^- was observed in the IR absorption spectra. This indicates that CH_3COO^- acts as a chelating agent at temperatures below 200 °C, preventing condensation reaction in the film, leading to the suppression of stress evolution.

$CH_3COCH_2COCH_3$ showed much more distinct effect in suppression of stress evolution. The film prepared with $CH_3COCH_2COCH_3$ had negligible stress up to 150 °C (Fig. 5), although the thickness was significantly reduced (Fig. 4). $CH_3COCH_2COCH_3$ may act as a chelating agent below 150 °C, suppressing the stress evolution. The great reduction in thickness may result just from solvent evaporation, where negligible condensation reaction occurs. Then, the stress steeply increased at temperatures over 150 °C (Fig. 5) where $CH_3COCH_2COCH_3$ is lost as is revealed in the IR absorption spectra.

As demonstrated above, chelating agents are effective in suppressing the stress evolution as far as they are present in films. When they are evaporated or decomposed, the stress increases drastically. Although the chelating agents are lost during heating, the porosity of the fired films calculated from the refractive index was 18.3 and 18.4% for those prepared with CH_3COOH and with $CH_3COCH_2COCH_3$, respectively, while 18.5% for that prepared without chelating agents. This indicates that chelating agents can suppress stress evolution without increasing the film porosity.

In all cases, the titania films were crystallized between 400 °C and 500 °C, while the stress significantly decreased over 400 °C or 450 °C (Fig. 5). It is not the microcracks that decreased the stress; no microcracks were detected in SEM images obtained after in situ stress measurement. This may be the stress relaxation that is promoted by accelerated atomic diffusion as will be discussed again in section "Residual Stress of Gel-Derived Coatings."

Effect of Methyltriethoxysilane

Methyltrialkoxysilanes are often mixed with tetraalkoxisilanes to prepare organic–inorganic thin films with methyl groups as the organic constituents, allowing the formation of thick silica-based films. Methyl groups directly bonded to silicon atoms are inert, not undergoing hydrolysis reaction. Therefore, they are expected to reduce stress evolution in the course of heating. Thin films were prepared from TEOS solutions containing $CH_3Si(OC_2H_5)_4$ (MTES), and the effect of MTES on stress evolution in films was investigated (Miyake 2003).

Starting solutions of mole ratios, MTES : TEOS : HNO_3 : H_2O : C_2H_5OH = x : (1-x) : 0.01 : 2 : 5, were prepared, where x = 0 or 0.6. The solutions were kept standing at 40 °C for 24 h and served as coating solutions. Spin coating was performed on Si(100) single-crystal wafers, where spinning rates of 2500 and 3000 rpm were employed for x = 0 and 0.6, respectively. Immediately after deposition, the gel films were subjected to in situ stress measurement.

Thickness of the films decreased as shown in Fig. 6. The extent of the reduction in thickness at 500 °C was not very different, 18% and 23% for x = 0 and 0.6, respectively. However, as seen in Fig. 7, the film prepared without MTES showed

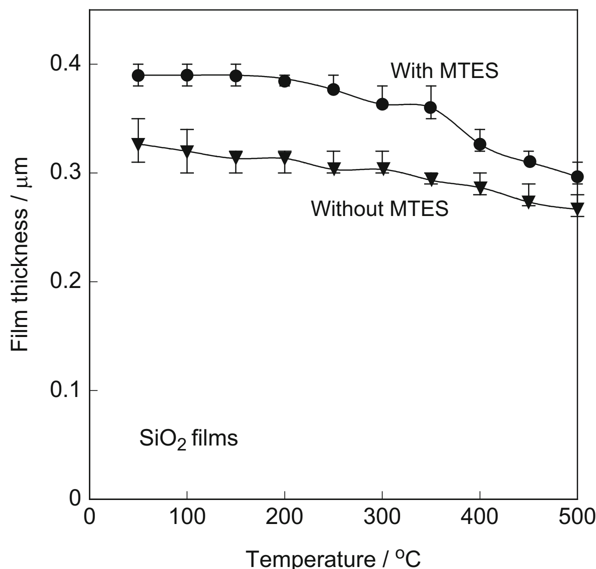

Fig. 6 Reduction in thickness on heat treatment for silica coatings prepared on single-crystal Si substrates from TEOS solutions with and without MTES (Miyake 2003)

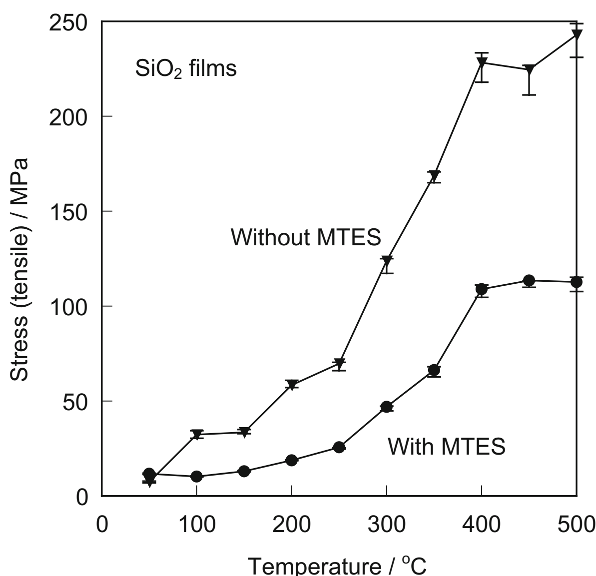

Fig. 7 Variation of in-plane stress as a function of temperature for silica coatings prepared on single-crystal Si substrates from TEOS solutions with and without MTES (Miyake 2003)

much lower tensile stress and much smaller slope in stress–temperature relation than that with MTES. IR absorption spectra revealed that the methyl groups remain in films at temperatures below 500 °C, where in situ stress measurement was conducted, and are decomposed between 500 °C and 600 °C. Therefore, the suppressed condensation reaction would be the cause of the lower degree of stress evolution in films prepared with MTES.

Effect of PVP

As will be described in section "Crack Formation in Gel-Derived Coatings," polyvinylpyrrolidone (PVP, Fig. 8) is effective in increasing the uncracking critical thickness of gel-derived ceramic thin films. In order to study the effect of PVP on stress evolution, in situ measurement of stress was conducted on titania gel films prepared from alkoxide solutions with and without PVP (Ishikawa and Kozuka 2004).

Starting solutions of mole ratios, $Ti(OC_3H_7^i)_4 : PVP : HNO_3 : H_2O : C_2H_5OH = 1 : x : 0.2 : 1 : 30$, where $x = 0$ or 0.5. The average viscosity molecular weight of PVP was 6.3×10^5, and the mole ratio for PVP was defined for the monomer. The starting solutions were kept in sealed glass containers at room temperature for 24 h and then were served as coating solutions. Spin coating was conducted on Si(100) single-crystal wafers at 4000 rpm.

The film prepared without PVP showed major reduction in thickness below 150 °C (Fig. 9), where the stress increased significantly up to 200 MPa (Fig. 10). The film prepared with PVP, on the other hand, showed an increase in stress only up to 70 MPa at 300 °C in spite of the large reduction in thickness by about 40% (Figs. 9 and 10). Then the stress increased largely at 300–380 °C where PVP was

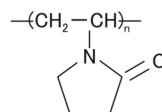

Fig. 8 Polyvinylpyrrolidone (PVP)

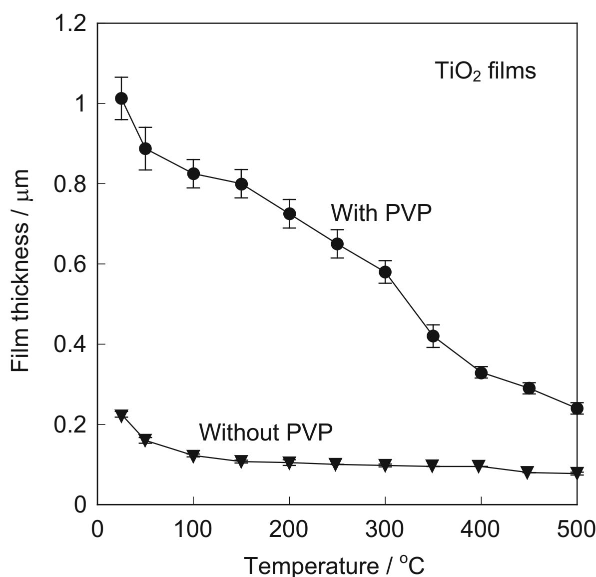

Fig. 9 Reduction in thickness on heat treatment for titania coatings prepared on single-crystal Si substrates from solutions with and without PVP (Ishikawa and Kozuka 2004)

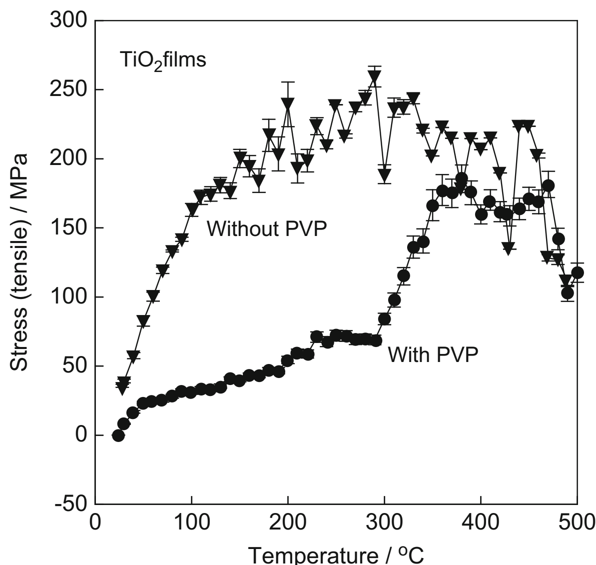

Fig. 10 Variation of in-plane stress as a function of temperature for titania coatings prepared on single-crystal Si substrates from solutions with and without PVP (Ishikawa and Kozuka 2004)

decomposed and/or oxidized. This clearly indicates that PVP in gel films prevents the stress evolution during heating. The C=O groups of PVP might coordinate the Ti atoms and/or make the hydrogen bonds with the OH groups of the metalloxane polymers, which is expected to hinder the condensation reaction in films and also allow plastic flow, suppressing the stress evolution in the heating-up stage. Besides, the smaller elastic constant of the film due to the incorporation of the organic polymer can also contribute to reduce the stress evolution.

XRD measurements revealed that the films are crystallized between 400 °C and 500 °C. The porosities calculated from the refractive index were 18.5% and 20.5% for the films prepared without and with PVP, respectively.

Crack Formation in Gel-Derived Coatings

Macroscopic Cracking versus Microscopic Cracking

Microcracks are occasionally observed in SEM images of the surface of ceramic coatings, which propagate along grain boundaries, when the film and the substrate have great difference in thermal expansion coefficient. Propagation of microcracks along grain boundaries (see zigzagged cracks in Fig. 11a) suggests that such cracks are formed at least after crystallization. Such microcracks can be prevented by matching the expansion coefficient (α) between the film and the substrate. For example, $BaTiO_3$ ($\alpha = 140 \times 10^{-7}\ K^{-1}$) films had microcracks when deposited on SiO_2 glass substrates ($\alpha = 5 \times 10^{-7}\ K^{-1}$) (Fig. 11a) while no microcracks on MgO single-crystal substrates ($\alpha = 135 \times 10^{-7}\ K^{-1}$) (Fig. 11b) (Kozuka et al. 2001a). A more serious problem annoying people in laboratories, however, is

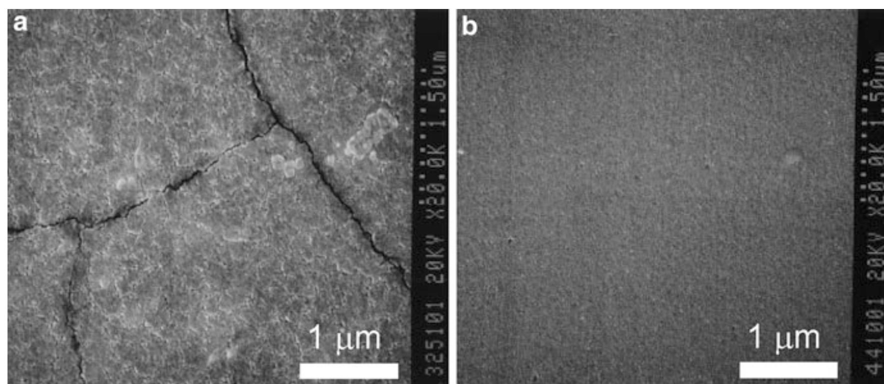

Fig. 11 Sol-gel-derived $BaTiO_3$ films deposited on (**a**) SiO_2 glass and (**b**) single-crystal MgO substrates (Kozuka et al. 2001a)

macroscopic cracking, which can be detected even with the naked eyes and is sometimes accompanied with film delamination. Such macroscopic cracking cannot be prevented even by matching the thermal expansion coefficient although many people believe it to occur due to mismatched expansion coefficient. Macroscopic cracking is liable to occur when thick gel films are fired. Then the cycles of gel film deposition and firing are needed while limiting the single-layer thickness under 0.1 µm. Such repetitive deposition, however, is time-consuming and impracticable in industries.

Table 2 summarizes the literature reporting macroscopic crack formation during gel film firing. The number of papers is small, and the cracks are always observed after firing the films. It seems almost sure that the intrinsic stress generating in the heating-up stage (not the thermal stress developing in the cooling-down stage) causes the macroscopic cracking as was discussed by Brinker et al. (1992). However, any experimental evidence had not been reported in literatures, and a very primitive question remained. When on the firing stage, i.e., the heating-up, annealing, or cooling-down stage, are the films cracked? It seems that this question had never been asked, and there was no confident answer, because cracks were usually observed after firing and cooling down the films. In order to make this point clear, in situ observation of cracking was made on gel films under heating (Kozuka 2002; Kozuka et al. 2003; Fujii 2002), which is described in the following sections.

In Situ Observation of Cracking

In any experiments described in the proceeding sections, the following experimental procedure was employed (Kozuka 2002; Kozuka et al. 2003; Fujii 2002). Alkoxide-derived gel films were deposited on single-crystal Si substrates (20 mm × 20 mm × (0.5–0.7) mm) by spin coating. Immediately after deposition, the gel films were heated at a constant rate up to 800 °C in a near-IR image furnace, and in situ

Table 2 Studies on cracking or delamination of sol-gel-derived coatings occurring on heat treatment (not including ours)

Film	Remarks	References
Silicate	Crack geometry, periodicity, and amplitude studied experimentally as a function of film thickness, curing time, and temperature	Sendova and Willis (2003)
SiO_2	Film thickness at the onset of cracking obtained. Initiation of cracks in the film propagating into the substrate observed. Crack energy release rate estimated	Chow et al. (2000)
SiO_2	Effect of volatile InP substrates studied. Crack patterns observed and theoretically analyzed	Liu et al. (2000)
CeO_2	Effect of film thickness studied. Crack spacing studied. Models examined	Atkinson and Guppy (1991)
SiO_2	Critical thickness as a function of water-to-alkoxide ratio and temperature studied	Garino (1990)
Calculation	Strain-energy release rates for delamination calculated	Thouless (1988)
Theory	Prediction of critical thickness by the film cracking number proposed	Evans et al. (1988)

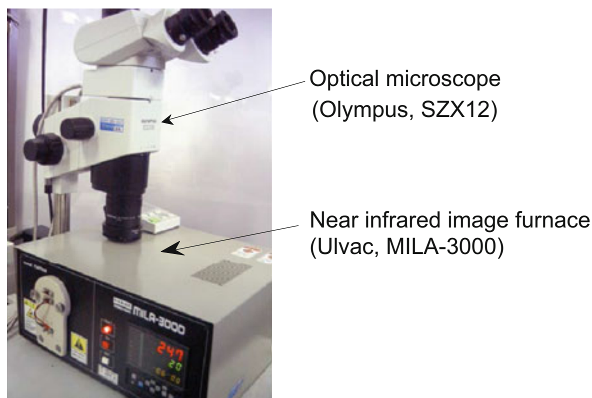

Fig. 12 Experimental setup for in situ observation of gel coating films during heating

observation was made at a magnification of 40 with an optical microscope through a window (Fig. 12). The temperature reading was calibrated beforehand by observing the melting of several compounds placed on the substrate.

Macroscopic Crack Formation in the Heating-Up Stage

Silica and titania gel films were prepared from solutions of molar compositions, $Si(OC_2H_5)_4 : H_2O : HNO_3 : C_2H_5OH = 1 : 4 : 0.01 : 4$ and $Ti(OC_3H_7^i)_4 : CH_3COCH_2COCH_3 : H_2O : i\text{-}C_3H_7OH = 1 : 2 : 1 : 5$, respectively (Kozuka 2002; Kozuka et al. 2003). In situ observation of cracking demonstrated that cracking does

occur in the heating-up stage at 100–400 °C, depending on the heating rate and film thickness as described in the following sections. This observation allows us to confirm that the tensile stress due to film densification causes the macroscopic cracking. It should also be noted that the titania thin films are crystallized at 400–500 °C, while cracked at lower temperatures; in other words, cracking took place prior to crystallization.

Effect of Thickness

The cracking onset temperature depended on the film thickness (Kozuka 2002, 2003c; Kozuka et al. 2003). Silica and titania gel films of various thickness were prepared from the solutions described in section "Macroscopic Crack Formation in the Heating-up Stage" by varying the spinning rate. Thicker films tended to be cracked at lower temperatures as seen in Fig. 13, where the cracking onset temperature is plotted against the final thickness. It is often experienced in laboratories that thicker films tend to cause macroscopic cracking. Now we can say more quantitatively that thicker films lead to cracking at lower temperatures although further study should be made on how the thickness can affect the intrinsic stress generating in the heating-up stage.

Effect of Heating Rate

The cracking onset temperature also depended on the heating rate (Kozuka 2002, 2003c; Kozuka et al. 2003). Silica and titania gel films were prepared from the

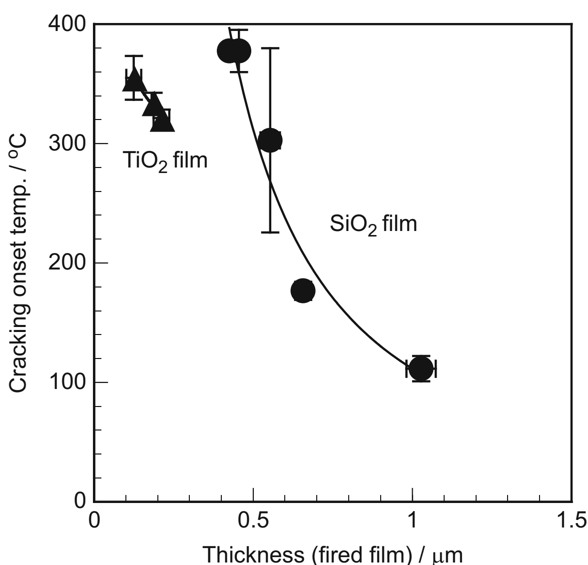

Fig. 13 Relationship between cracking onset temperature and final film thickness obtained on silica and titania gel films deposited on single-crystal Si substrates and heated at 100 °C min^{-1} (Kozuka 2002; Kozuka et al. 2003)

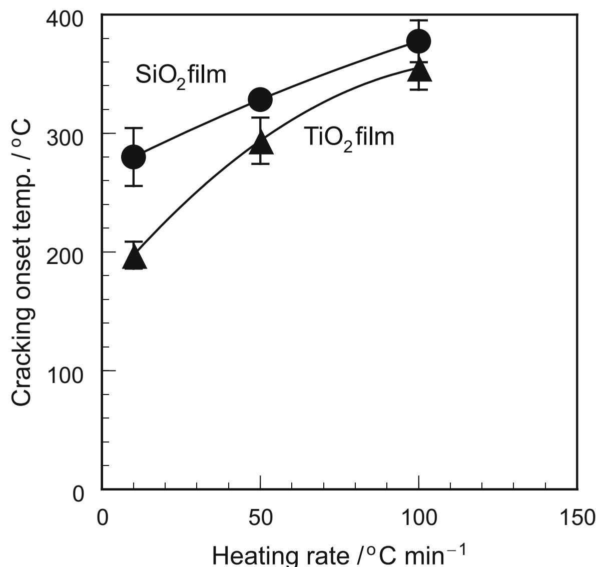

Fig. 14 Relationship between cracking onset temperature and heating rate obtained on silica and titania gel films deposited on single-crystal Si substrates (Kozuka 2002; Kozuka et al. 2003)

solutions described in section "Macroscopic Crack Formation in the Heating-up Stage" at 1800 and 3440 rpm, respectively, and heated at various rates. Cracking occurred at higher temperatures when the films were heated at higher rates as shown in Fig. 14, where the cracking onset temperature is plotted against heating rate. Generally, lower heating rates tend to cause macroscopic cracking as is experienced in laboratories, and now we can say more quantitatively that cracking occurs at lower temperatures at lower heating rates. We also found that lower heating rates result in lower porosities of films on the basis of the refractive index measurement. This indicates that lower heating rates can provide enough time for the films to be densified during heating, leading to higher tensile stress in the plane of the substrate.

Effect of the Amount of Water for Hydrolysis

Solutions of mole ratios, TEOS : H_2O : HNO_3 C_2H_5OH = 1 : x : 0.01 : 4, were prepared where $x = 2$, 4, and 10, kept in sealed glass containers at 30 °C for 24 h and served as coating solutions (Kozuka and Komeda 2004). Spin coating was performed at 500 or 900 rpm, and the gel films were heated at 10 °C min^{-1} up to 800 °C. The final film thickness was about 0.9–1.1 μm, 0.95 μm, and 1.4–1.8 μm at H_2O/TEOS = 2, 4, and 10, respectively, at a spinning rate of 500 rpm and was 0.7–0.8 μm, 0.7 μm, and 0.5–0.6 μm at H_2O/TEOS = 2, 4, and 10, respectively, at a spinning rate of 900 rpm. All the films were cracked on heating except for those prepared from the solution of H_2O/TEOS = 2 at 900 rpm.

The cracking onset temperature thus defined is plotted versus H_2O/TEOS mole ratio in solution in Fig. 15. In spite of the distribution of data, the cracking onset

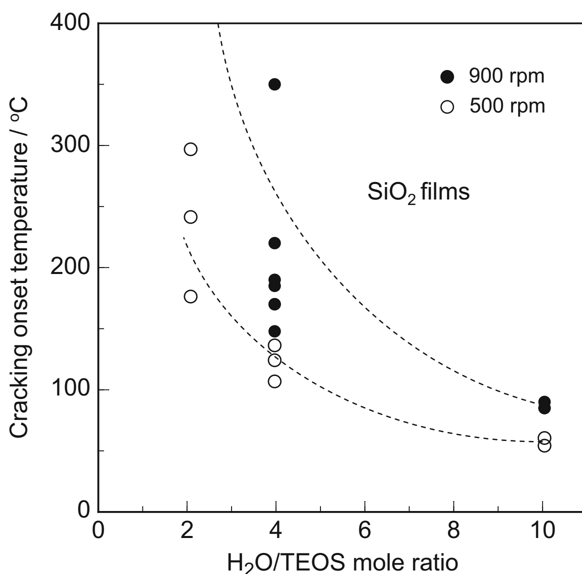

Fig. 15 Cracking onset temperature plotted against H_2O/TEOS mole ratio in solutions obtained on silica gel films deposited on single-crystal Si substrates and heated at 10 °C min^{-1} (Kozuka and Komeda 2004)

temperature appeared to decrease with increasing H_2O/TEOS ratio in solutions. This agrees qualitatively with Gario's report (Garino 1990), where the uncracking critical thickness of alkoxide-derived silica coatings was found to decrease with increasing H_2O/alkoxide ratio in solutions. The higher stress at higher H_2O/TEOS ratios described in section "Effect of the Amount of Water for Hydrolysis" would be the origin of the lower cracking onset temperatures. The higher spinning rate of 900 rpm, i.e., the smaller thickness, leads to higher cracking onset temperatures, which agrees with what is described on the thickness dependence on cracking onset temperature in section "Effect of Thickness."

The shape of the cracks could be classified roughly into three groups, (i) scalelike shape (Fig. 16a), (ii) wormlike shape (Fig. 16b), and (iii) linear shape (Fig. 16c), where the photographs were taken at room temperature after in situ observation experiments. The thickness of the films tended to be larger near the edge of the substrate, and the film near the edge was more liable to be cracked than that at the center. Fig. 16b is a photograph taken near the edge on the sample that was not cracked in the center, where the arrow denotes the direction toward the substrate center. It is seen that the wormlike cracks are observed near the edge, which change into linear-shaped ones toward the center.

The shape of the cracks had a tendency to shift from scalelike to wormlike and then to linear shape as the cracking onset temperature increases. In other words, cracks are likely to propagate curled at lower temperatures and straight at higher temperatures. As the heating temperature increases, the stiffness of the gel films increases as a result of the condensation reaction in films and its densification. This could make the film brittle, allowing the cracks to propagate in straight direction. On the other hand, at lower temperatures, the three-dimensional network is not yet

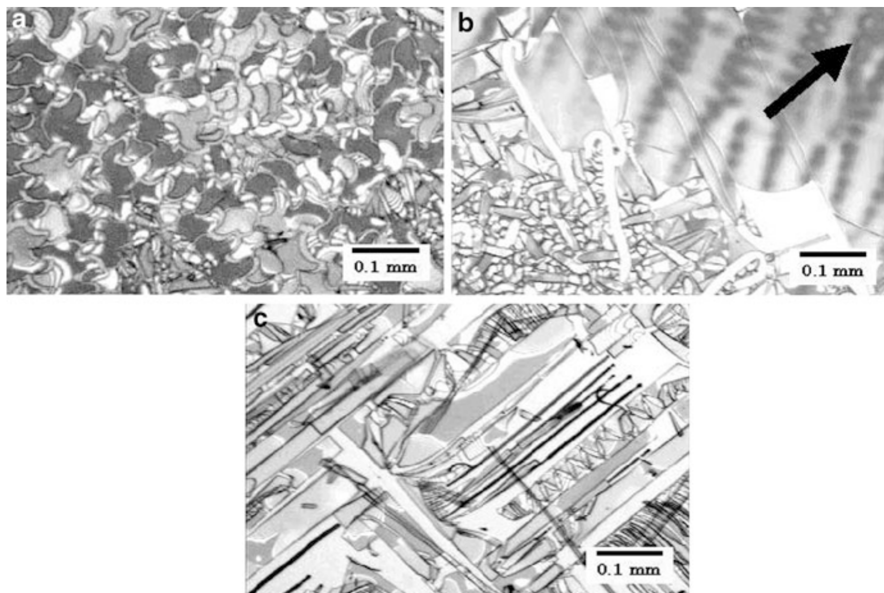

Fig. 16 Photographs of the silica thin films heated at a rate of 10 °C up to 800 °C and cooled down to room temperature in the near-IR image furnace. The films were prepared on single-crystal Si substrates from solutions of (**a**) H_2O/TEOS = 4 at 500 rpm, (**b**) H_2O/TEOS = 10 at 900 rpm, and (**c**) H_2O/TEOS = 4 at 900 rpm. The cracking onset temperature measured at the center of the film surface was (**a**) 60 °C and (**c**) 350 °C. For (**b**) no cracking was observed at the center, and the photograph was taken near the substrate edge. The arrow indicates the direction toward the center

developed, and the films still retain plasticity. This could provide freedom in direction of crack propagation, leading to scalelike-shaped cracks.

Effect of Humidity

Sol-gel deposition in humid days often results in macrocrack formation on firing as is experienced in laboratories. In order to know how the relative humidity affects the cracking behavior, in situ observation was made on alkoxide-derived silica gel films deposited and heated at different relative humidities (Fujii 2002). A solution of mole ratios, TEOS : H_2O : HNO_3 C_2H_5OH = 1 : 4 : 0.01 : 4, was prepared, kept in sealed glass containers at room temperature for 1 h, and served as coating solution. Immediately after deposition, the gel film was heated at 10 °C min^{-1} up to 800 °C in a near-IR furnace. The spin coater and the near-IR image furnace were placed in a glove box, and the gel film deposition, heating, and in situ observation were conducted in a controlled humidity.

Cracking onset temperature is plotted versus relative humidity in Fig. 17. At any spinning rate, the cracking onset temperature decreased with increasing relative humidity. In other words, when gel films are deposited and heated at higher relative

Fig. 17 Relationship between cracking onset temperature and relative humidity obtained on silica gel films prepared on single-crystal Si substrates and heated at 10 °C min^{-1}

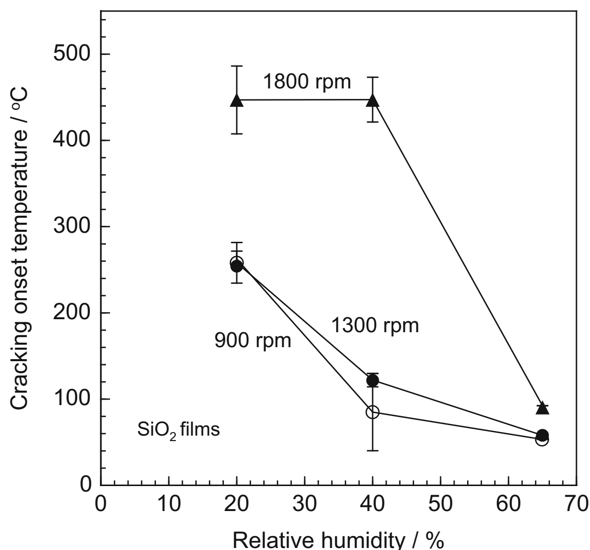

humidities, cracking is likely to occur at lower temperatures. Difference in final thickness and porosity was very small between the films deposited and heated at different humidities. In other words, no distinct difference in densification behavior could be obtained.

The reason for the lowered cracking onset temperature at higher humidity is not known. However, there are some possible reasons. One is the hydrolysis reaction at the gel film surface that is promoted by water vapor in the atmosphere, leading to the condensation reaction at the surface and the generation of stress gradient across the thickness direction. Second, the capillary pressure is increased at the film surface due to the adsorption of water, resulting in an increase in tensile stress. Further study on the effect of humidity on stress generation should be made by means of in situ measurement of stress in films under controlled humidity.

Strategy for Thick Film Formation without Macroscopic Cracking

Thick Film Formation via Non-cycled Deposition in Literature

As is often experienced in laboratories, thick gel coatings are liable to undergo macroscopic cracking during firing. The maximum thickness achievable without cracking via non-cycled deposition is often called “uncracking critical thickness” and is normally less than 100 nm for ceramic thin films. Thin film devices, on the other hand, often need thickness over submicron so that they have desired properties or functions. Then, in order to achieve desired thickness, gel film deposition and firing are cycled in laboratories, while the single-layer thickness is limited under the critical thickness; when the thickness of the single layer is 50 nm, for instance,

Table 3 Thick film formation via non-cycled deposition in literature

Film	Single-layer thickness achieved	Remarks	References
PZT	>1 μm	Diethanol amine added as chelating agent	Ohya et al. (2002)
PZT	3 μm	PZT powders added. Diethanol amine added as chelating agent	Ohya et al. (2002)
PZT	0.83 μm	Diol-based solutions	Maki et al. (2001)
PZT	0.5–1 μm	Diol-based solutions	Arscott et al. (1997), Tu et al. (1996), Tu and Milne (1995a), Tu and Milne (1995b)
PZT	0.4 μm	Triol-based solutions	Sriprang et al. (2000), Arscott et al. (1999)
(Pb, Ca) TiO_3	0.5 μm	$Ti(OC_3H_7)_2(CH_3COCHCOCH_3)_2$	Chewasatn and Milne (1997)
ITO	0.5 μm	Crystalline nanoparticles redispersed in an ethanol solution containing hydrolyzed organosilanes	Al-Dahoudi and Aegerter (2002), Al-Dahoudi et al. (2001)
ZnO	0.8–2 μm	ZnO colloids	Hilgendorff et al. (1998)
SiO_2	2 μm	$CH_3(OC_2H_5)_4$ added to TEOS solutions	Innocenzi et al. (1994)
C_{60}-doped SiO_2	10–100 μm	3-Glycidoxypropyltrimethoxysilane	Innocenzi et al. (2000)

20 cycles of deposition should be conducted to obtain 1 μm-thick films. Such repetitive deposition is not realistic in industries.

The strategy to prevent the macroscopic cracking is to suppress the tensile stress that is generated in the heating-up stage as is clear from the descriptions in sections "Stress Evolution in Gel Films During Heating" and "Crack Formation in Gel-Derived Coatings." This could be achieved by promoting structural relaxation or plastic flow in films. This strategy has already been proposed by Brinker et al. (Brinker et al. 1992), and examples are found in literatures (Table 3), where the organic modification of alkoxide precursors, the chelation by multidentate ligands, and the addition of nano-sized particles in solutions are proposed.

Polyvinylpyrrolidone for Thick Film Formation

Saegusa and Chujo (Saegusa and Chujo 1990, 1992) have demonstrated that organic polymers with amide groups such as PVP can be hybridized with metalloxane polymers in molecular scale through strong hydrogen bonds between the C=O groups of the former and the OH groups of the latter. The author thought that such

Table 4 Thick film formation aided by PVP. P_r, E_c, and ϵ' are remanent polarization, coercive field, and dielectric constant, respectively

Film	Single-layer thickness achieved	Remarks	References
$BaTiO_3$	0.56 μm	Transparent; $\varepsilon' = 290$; sols stable in viscosity	Kozuka and Higuchi (2001, 2003), Kozuka et al. (2003)
$BaTiO_3$	0.77 μm	Transparent; $\varepsilon' = 310$; sols stable in viscosity	Kozuka et al. (2004)
$BaTiO_3$	1.2 μm	Transparent	Kozuka and Kajimura (1999, 2000), Kozuka et al. (2000)
$BaTiO_3$	2.1 μm	Transparent	Kozuka et al. (2001b, 2003)
PZT	2 μm	Porous and opaque	Kozuka et al. (2001c), Kozuka and Takenaka (2002)
PZT	0.75 μm	Transparent; $P_r = 25$ μC cm^{-2}; $E_c = 96$ kV cm^{-1}; sols stable in viscosity	Takenaka and Kozuka (2001), Kozuka (2002), Kozuka et al. (2003)
PZT	2.2	Slightly opalescent; $P_r =$ 21 μC cm^{-2}; $E_c = 90$ kV cm^{-1}; $\varepsilon' = 370$	Kozuka et al. (2004)
$BaBi_4Ti_4O_{15}$	0.9 μm	Opalescent	Nakai and Kozuka (2004)
$BaBi_4Ti_4O_{15}$	0.4 μm	Slightly opalescent; $\varepsilon' = 380$	Kozuka et al. (2004)
Fe_2O_3	0.9 μm	Transparent	Kozuka et al. (2001b)

C=O groups could work as the capping agent for the OH groups of the metalloxane polymers, suppressing the condensation reaction and promoting the structural relaxation. Based on the idea, the author's group prepared ceramic thin films from alkoxide solutions containing PVP and demonstrated that PVP can increase the uncracking critical thickness as summarized in Table 4.

Barium titanate gel films were prepared on silica glass substrates using solutions of molar compositions, $Ba(CH_3COO)_2 : Ti(OC_3H_7^i)_4$: PVP : $CH_3COOH : H_2O$: i-$C_3H_7OH = 1 : 1 : (0–1) : 9.08 : 20 : 20$. PVP of average viscosity molecular weight of 6.3×10^5 was employed, and the mole ratio for PVP was defined for monomers (Kozuka et al. 2001b, c; Kozuka 2003). The thickness of the gel films was varied by varying the substrate rotation or withdrawal speed in spin and dip coating, respectively. The gel films thus obtained were fired at 700 °C, and the macroscopic cracking was examined after cooling. As seen in Fig. 18, the critical thickness was 0.2 μm without PVP in sols, while it increased up to 2 μm when PVP was added in sols at a mole ratio of PVP/titanium alkoxide of 0.5. As demonstrated, PVP in gel films can increase the critical thickness of sol-gel-derived ceramic coatings. The increased critical thickness is achieved by the suppressed stress evolution in the heating-up stage as was demonstrated in section "Stress Evolution in Gel Films During Heating." The maximum thickness achieved so far without cracking via

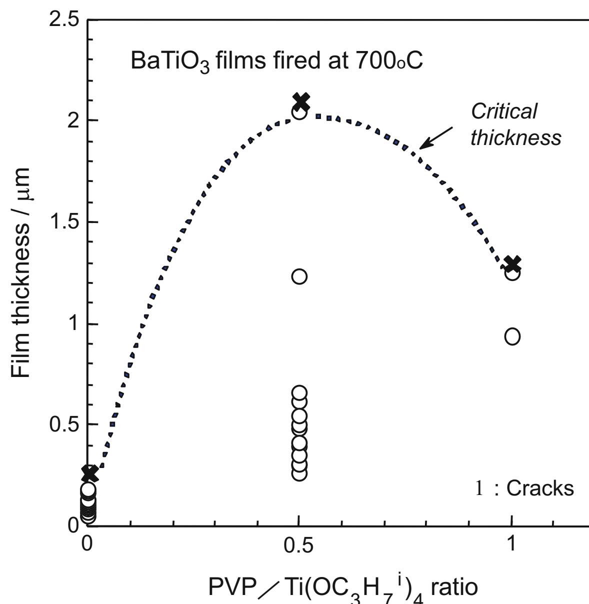

Fig. 18 Presence and absence of macrocracks in barium titanate films prepared via non-cycled deposition on silica glass substrates with varying spinning and withdrawal speed and fired at 700 °C (Kozuka et al. 2001b, c; Kozuka 2003)

single-step deposition is 2.1 μm for $BaTiO_3$ (Kozuka et al. 2001b, 2003), 2.0 μm for PZT (Kozuka et al. 2001c; Kozuka and Takenaka 2002), 0.9 μm for $BaBi_4Ti_4O_{15}$ (Nakai and Kozuka 2004), and 0.9 μm for Fe_2O_3 (Kozuka et al. 2001b) films.

Thermal analysis and IR absorption spectroscopy indicated that PVP in gel films are thermally decomposed and oxidized around 250–400 °C, where significant reduction in thickness is observed. It was demonstrated in section "Stress Evolution in Gel Films During Heating" that PVP does not increase the porosity of the fired films, where thickness was limited to 0.25 μm. However, this is not the case with thicker films. The decomposition of PVP provides porosity for films with final thickness over submicron, which, however, are optically transparent in many cases (Table 4). Although the porosity is not measured, the porous nature of the films is revealed in the following experimental facts (Kozuka et al. 2001b; Kozuka 2002). Gel films were deposited on silica glass substrates using a sol prepared from a solution of mole ratio, $Ba(CH_3COO)_2$: $Ti(OC_3H_7^i)_4$: PVP : H_2O : CH_3COOH : $C_3H_7^iOH$ = 1 : 1 : 1 : 20 : 9.08 : 20. When the gel film was fired at 700 °C, a 1.2 μm-thick $BaTiO_3$ film resulted via non-cycled deposition as shown in Fig. 19a. When the gel film was heated stepwise at 300 °C, 500 °C, and 700 °C, on the other hand, the thickness decreased down to 0.7 μm as seen in Fig. 19b, and higher optical transmittance was found. These indicate that the 1.2 μm-thick $BaTiO_3$ film fired at 700 °C was porous and not fully dense but also suggest that higher densities can be achieved by slower PVP decomposition.

Although the resultant films are not always fully dense, a 0.77 μm-thick $BaTiO_3$ film could be obtained via non-cycled deposition, having a dielectric constant of 310 at 1 kHz (Table 4) (Kozuka et al. 2004), which is comparable with those reported

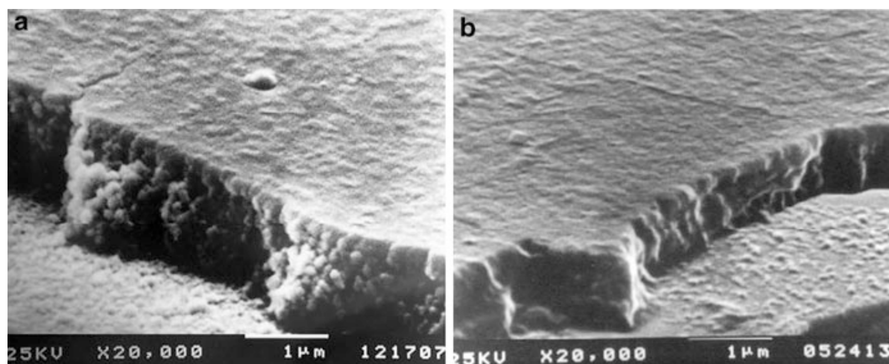

Fig. 19 SEM pictures of fired $BaTiO_3$ films prepared via non-cycled deposition on silica glass substrates using a sol containing PVP and heated (**a**) at 700 °C and (**b**) stepwise at 300°, 500°, and 700 °C for 10 min (Kozuka 2001e, 2002)

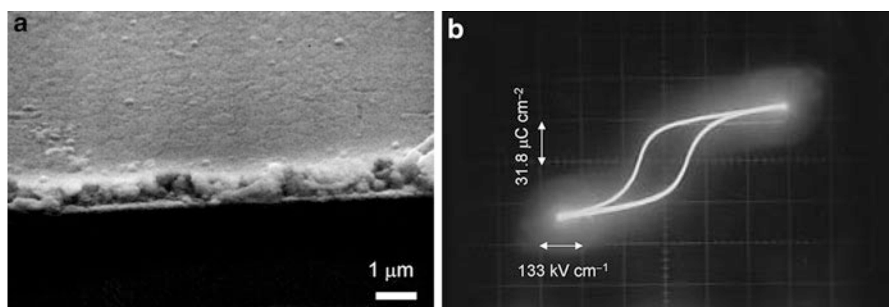

Fig. 20 (**a**) SEM picture and (**b**) P–E hysteresis loop of a 0.75 μm-thick PZT film prepared via non-cycled deposition from a solution containing PVP (Takenaka and Kozuka 2001; Kozuka et al. 2003)

in literatures on gel-derived $BaTiO_3$ films prepared via cycled deposition. Also 0.75 μm-thick PZT films (Fig. 20a) exhibited *P–E* hysteresis loops (Fig. 20b), where remanent polarization and coercive field were 25 μC cm^{-2} and 96 kV cm^{-1}, respectively (Table 4) (Takenaka and Kozuka 2001; Kozuka et al. 2003). Both of the solutions were stable in viscosity at room temperature over 1000 h, which is another benefit for fabricating ceramic coatings in industrial scale.

PVP was also found to greatly assist the formation of complex oxides in single phase on firing, while in conventional sol-gel method, double or triple alkoxides should be synthesized so that desired complex oxides are crystallized in single phase. This is another great benefit of PVP for preparing functional ceramic coating films. The C=O groups of PVP could coordinate the metal atoms of alkoxides, possibly leading to the homogeneous distribution of the elements in solutions.

Residual Stress of Gel-Derived Coatings

As mentioned in section "Introduction," we have to clarify the effects of the processing parameters on the residual stress for sol-gel-derived oxide thin films in order to obtain a guideline for residual stress control, which is important from the viewpoint of their technological use. The most fundamental parameters that would affect the residual stress are the heat-treatment temperature and time, which should always be configured in actual processing. Systematic experimental data on the relationship between residual stress and heat-treatment conditions may provide us a clear picture on the residual stress development during film formation.

A few papers have been published on the effects of heat-treatment conditions on the residual stress of sol-gel-derived thin films. Syms measured the in-plane residual stress of P_2O_5-doped SiO_2 films that were deposited on Si substrates as a function of annealing temperature of 900–1150 °C, and showed that the residual stress is compressive, increasing with increasing annealing temperature (Syms 1994b). Mehner et al. studied the in-plane residual stress of ZrO_2 films on stainless substrates in an annealing temperature range of 600–750 °C, showing that the tetragonal-to-monoclinic phase transformation induces compressive residual stress (Mehner et al. 1997). Brenier et al. studied the in-plane residual stress of ZrO_2 films as a function of annealing temperature up to 400 °C on glass plates (Brenier et al. 1999; Brenier 2002). They demonstrated that the stress is tensile, increasing with increasing annealing temperature, and that the slope of stress-annealing temperature curves increases when acetylacetone, a chelating agent, is decomposed. Corkovic et al. reported the in-plane residual stress of $Pb(Zr,Ti)O_3$ on platinized (100) silicon wafers as a function of annealing temperature up to 550 °C, showing that the stress is compressive at lower annealing temperatures, turning out to be tensile at higher annealing temperatures (Corkovic et al. 2008).

In spite of these efforts, the heat-treatment temperature range had been limited, and the clear picture on the residual stress development remained to be given. Then the author's group studied the in-plane residual stress of yttria-stabilized zirconia (YSZ) films that were deposited on Si(100) wafers and heated at a wide range of annealing temperature (100–950 °C) (Ohno et al. 2012). YSZ was chosen because the crystalline phase is cubic irrespective of the annealing temperature, and hence the effect of crystalline phase transformation needs not be taken into account.

A starting solution of mole ratio, $Y(NO_3)_3 \cdot 6H_2O : Zr(OC_3H_7^n)_4 : HNO_3 : H_2O : C_3H_7^nOH = 0.2 : 0.8 : 0.2 : 0.315 : 20$, was prepared, and spin coating was conducted on Si(100) wafers. The gel films thus obtained were fired at 100–950 °C for 10 min and served as the samples for the residual stress measurement. The as-deposited gel films were also served for the in situ stress measurement during heating.

When the gel film was heated, the thickness decreased significantly with increasing heat-treatment temperature up to 500 °C and very slightly decreased or remained almost constant over 500 °C as seen in Fig. 21. The great reduction in thickness may have resulted from the solvent evaporation, the nitrate decomposition, and the

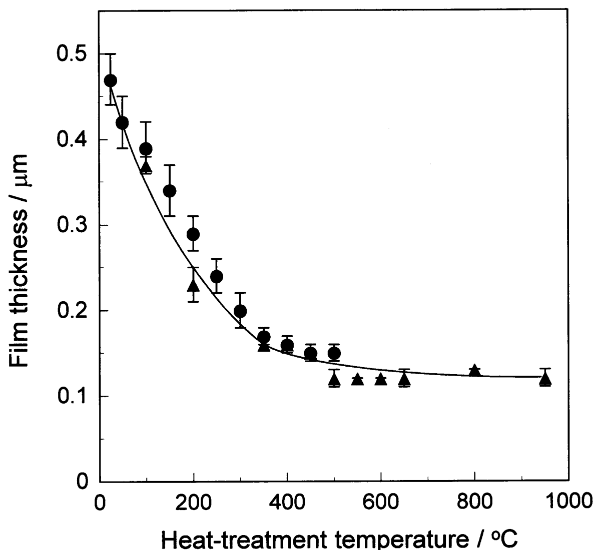

Fig. 21 Film thickness plotted versus heat-treatment temperature. The gel films were heated at different temperatures (▲) or heated successively up to 500 °C at intervals of 50 °C (●). Each heat treatment was conducted for 10 min (Ohno et al. 2012)

condensation reaction in the film. The XRD measurement revealed that the film is crystallized into cubic zirconia at 400–500 °C (Fig. 22).

Figure 23 shows the residual in-plane stress plotted versus heat-treatment temperature. The residual stress showed rather complex dependence on the heat-treatment temperature. It became compressive at heating temperatures of 100–200 °C, turned out to be tensile around 350 °C, and increased with increasing firing temperature up to 500 °C, where the film was crystallized. The tensile residual stress slightly decreased around 600 °C and increased again over 600 °C.

In order to understand such complex dependence, the as-deposited gel film was also subjected to the in situ measurement of intrinsic stress during heating, the result of which is shown in Fig. 24. It should be noted that the horizontal axis in Fig. 24 represents the temperature where the stress was measured, while that in Fig. 23 shows the firing temperature. The upper temperature in Fig. 24 is limited to 500 °C, which is the maximum temperature that can be achieved by the stress-measurement apparatus. As seen in Fig. 24, the intrinsic stress was negligible at room temperature, while it became tensile and increased with increasing temperature, slightly decreasing at around 425 °C.

Based on the intrinsic stress–temperature curve (Fig. 24), we tried to understand the dependence of the residual stress on the heat-treatment temperature (Fig. 23). The residual stress became compressive when the film was heated at 200 °C (Fig. 23). On the other hand, the film had tensile intrinsic stress at 200 °C as seen in Fig. 24. This situation is represented in arrow (ii) in Fig. 25, where the stress is plotted versus temperature, and all the residual stress values are plotted at room temperature (all the data are transferred from Figs. 23 and 24). As represented in arrow (ii) in the figure, the stress changed from tensile to compressive when the film

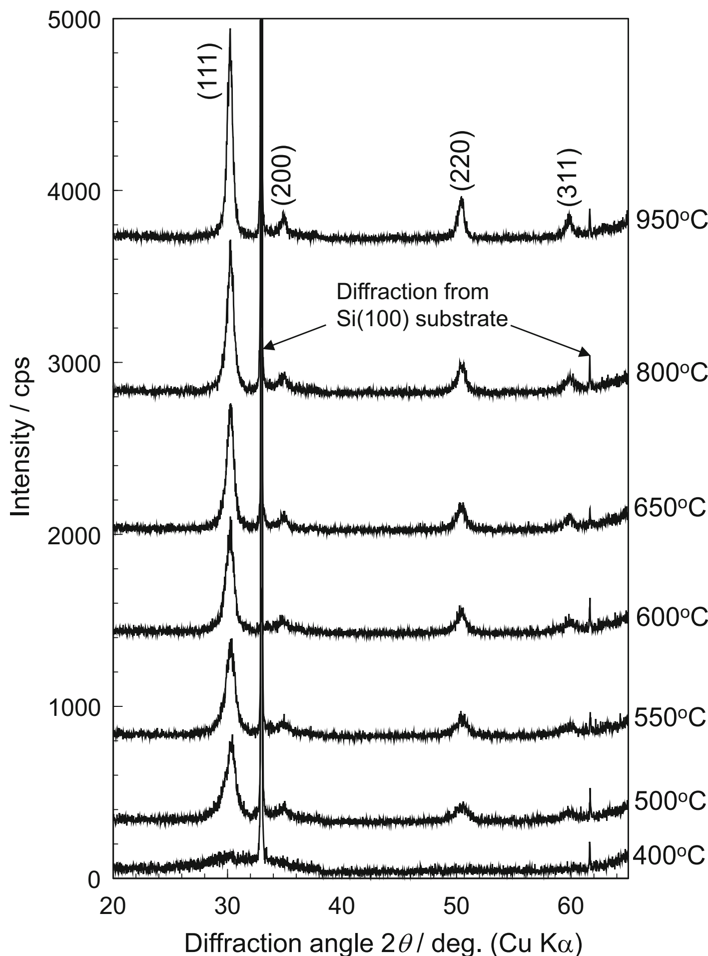

Fig. 22 XRD patterns of the films fired at various temperatures for 10 min (Ohno et al. 2012)

was cooled from 200 °C to room temperature. Considering that the gel film may have larger thermal expansion coefficient than the silicon substrate, the tensile-to-compressive change cannot be attributed to the thermal stress generated in the cooling-down stage. Such a behavior was not observed in purely alkoxide-derived titania or silica thin films (not shown here). The nitrate as a part of the precursor may have some role, but the details are unknown and should be studied in the future.

The residual stress turned out to be tensile at a heat-treatment temperature around 350 °C and increased with increasing heat-treatment temperature up to 500 °C (Fig. 23). This may be caused in principle by the increase in intrinsic stress that results from film densification (Fig. 24). However, there is another cause. As shown by the arrows (iii)–(vi) in Fig. 25, when the firing temperature is increased from 350 °C to 500 °C, the variation of stress during cooling drastically changes, i.e., from

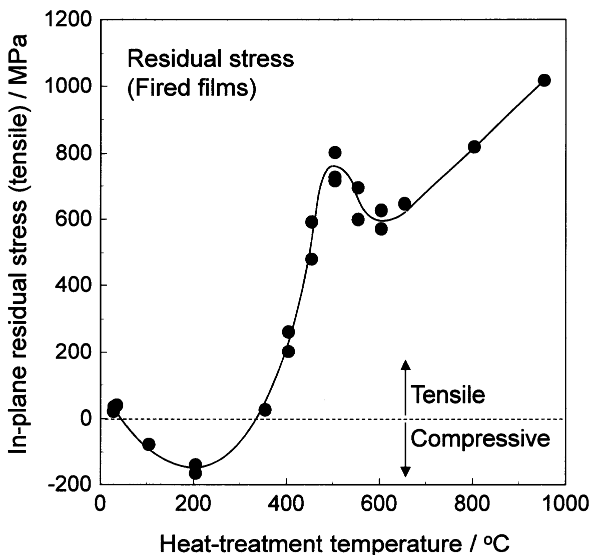

Fig. 23 In-plane residual stress of the fired films measured at room temperature as a function of heat-treatment temperature. The heat treatment was conducted at each temperature for 10 min (Ohno et al. 2012)

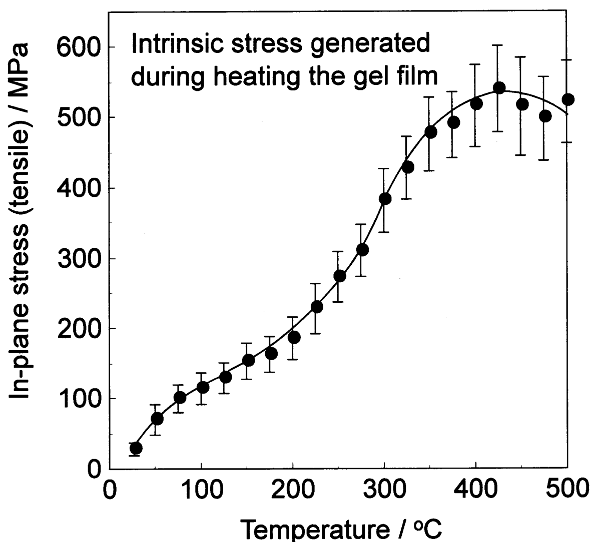

Fig. 24 In-plane intrinsic stress for the gel film measured in situ during heating at 5 °C min^{-1}. In order to assess the standard deviation of ΔR, the sample preparation and the deflection measurement were conducted three times (Ohno et al. 2012)

downward to upward. Such a change can be explained by the reduction in structural relaxation. When the film is fired at higher temperatures, the condensation reaction proceeds, which hinders the structural relaxation during cooling. In such a situation, the thermal stress that develops during cooling, which is tensile due to the larger expansion coefficient of the film, becomes evident, which also contributes to the variation of stress during cooling from downward to upward.

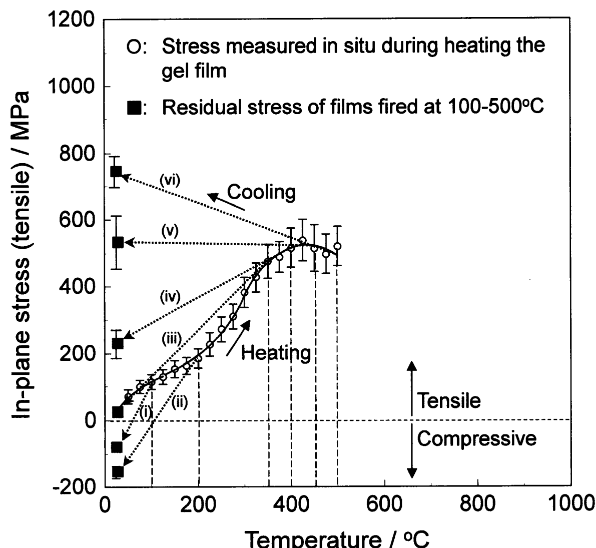

Fig. 25 Stress–temperature curves showing how the residual stress is developed for films fired at temperatures below 500 °C. The intrinsic stress developed during heating (○) and the residual stress (■) were taken from Figs. 24 and 23, respectively. All the residual stress values are plotted at room temperature (Ohno et al. 2012)

In summary, the increase in tensile residual stress observed at firing temperatures of 200–500 °C (Fig. 24) can be attributed to (a) the increase in tensile intrinsic stress (Fig. 23) as well as to (b) the reduced structural relaxation and (c) the increased tensile thermal stress occurring during cooling, all of which result from the film densification.

At firing temperatures of 500–600 °C, the residual stress slightly decreased with increasing firing temperature (Fig. 24). For understanding such a behavior, the information on intrinsic stress at 500–600 °C is strongly desired. However, no intrinsic stress data over 500 °C is available because the apparatus has an upper-limit temperature. Then we estimated the intrinsic stress over 500 °C in the following manner.

We measured the stress in situ during heating and cooling for the films that were fired at temperatures over 500 °C, the results of which are shown in Fig. 26. Nearly reversible stress variation was seen during heating and cooling. Then we estimated the intrinsic stress over 500 °C by extrapolating these stress–temperature curves at such high temperatures. Such extrapolation and estimated intrinsic stress values are illustrated in Fig. 27, where the closed symbols are taken from Fig. 26 and the estimated intrinsic stress values are shown as double circles. When the gel film is heated up to 950 °C, for instance, and then cooled down to room temperature, the stress may follow the curve in the orders (i), (ii), (iii), (iv), and (v) in Fig. 27, resulting in the residual stress of about 1000 MPa at room temperature.

As seen in Fig. 27, the intrinsic stress increases and then decreases with increasing temperature. The decrease in stress may result from the activated atomic diffusion, which allows the structural and stress relaxation to occur. (Another cause of the apparent reduction in intrinsic stress is the emergence of thermal stress. When the

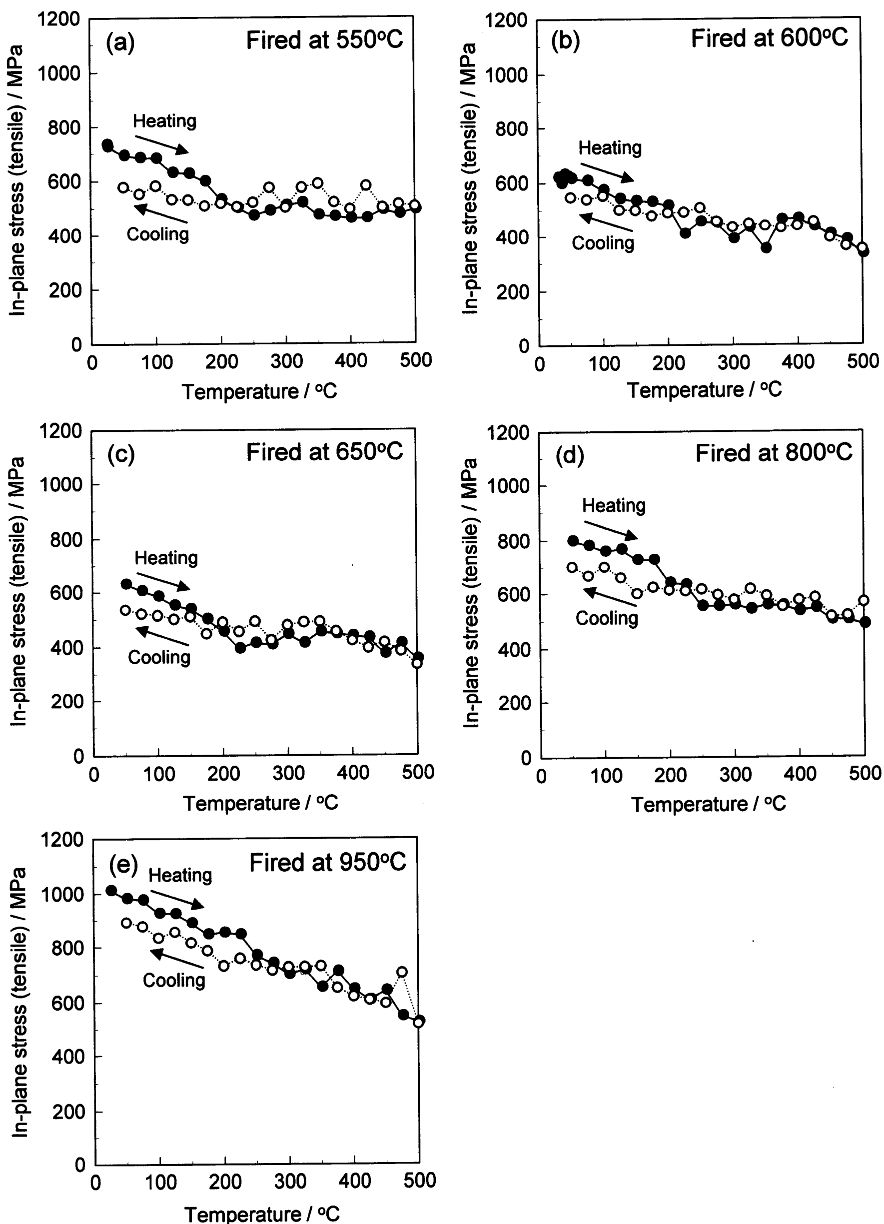

Fig. 26 Stress measured in situ during heating and cooling for the fired films. The films were fired at (**a**) 550, (**b**) 600, (**c**) 650, (**d**) 800, and (**e**) 950 °C before the stress measurement. The closed and open symbols represent the stress measured during heating and cooling, respectively. The heating and cooling rates in the stress measurement were 5 °C min^{-1}, but at low temperatures, the cooling rate was smaller than 5 °C min^{-1} because of the heat capacity of the stress-measurement apparatus (Ohno et al. 2012)

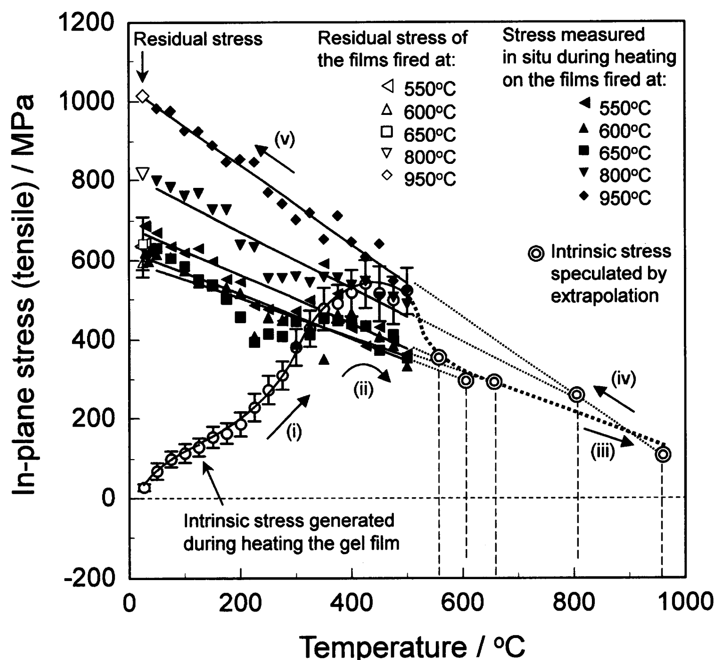

Fig. 27 Stress–temperature curves show how the residual stress is developed for films fired at temperatures over 500 °C. The intrinsic stress developed during heating up to 500 °C (O) was taken from Fig. 24. The closed symbols represent the stress values measured in situ during heating the fired films, taken from Fig. 26. The intrinsic stress of the films at their firing temperatures (>500 °C) was estimated by extrapolating the closed symbol lines and represented by double circles. All the residual stress values are plotted at room temperature (Ohno et al. 2012)

films are densified, the thermal stress, which must be compressive during heating, may be manifested. Such an emergence of compressive stress may also contribute to the decrease in intrinsic (tensile) stress.) It is seen that the intrinsic stress decreases from 500 to 300 MPa when the firing temperature is increased from 500 °C to 600 °C. Such a reduction in intrinsic stress may be the cause of the decrease in residual stress observed in Fig. 24.

The residual stress increased again with increasing firing temperature over 600 °C (Fig. 24) although the estimated intrinsic stress decreased with increasing temperature (Fig. 27). As seen in Fig. 27, the tensile thermal stress (the slope of the closed marks) generated during cooling increased with increasing firing temperature over 600 °C. Such an increase in thermal stress generated during cooling may have caused the increase in residual stress.

Then, what is the cause of the increase in thermal stress during cooling? Figure 28a, b show the integrated intensity of YSZ (111) and (220) XRD peaks and the crystallite size, respectively, plotted versus firing temperature. It is seen that both the XRD peak area and the crystallite size increase with increasing firing temperature. The former

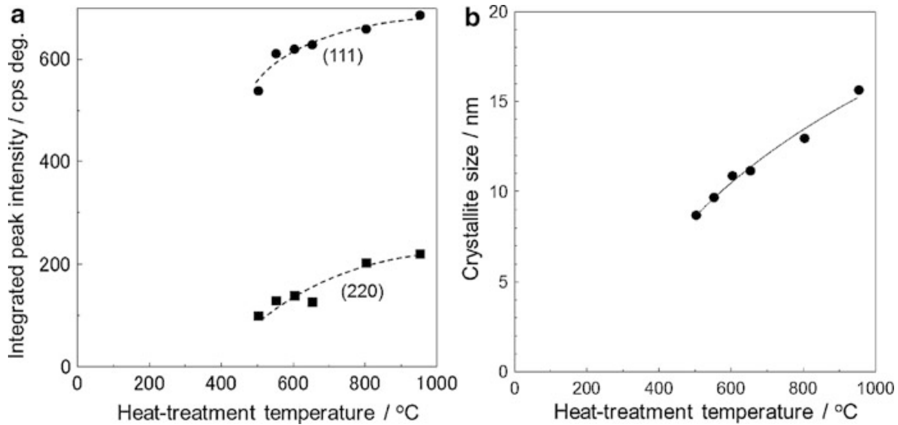

Fig. 28 (**a**) Integrated intensity of (111) and (220) peaks and crystallite size plotted versus firing temperature. The crystallite size was determined from the full width at half maximum of the (111) peak (Ohno et al. 2012)

reveals the increase in volume fraction of the crystalline phase, and the latter suggests the reduction in grain boundaries. Both of these could result in an increase in Young's modulus of films, resulting in an increase in thermal stress.

In summary, the increase in residual stress observed at firing temperatures over 600 °C is attributed to the increase in thermal stress generated during cooling due to the progress of the crystallization and grain growth.

Finally, a model is given in Fig. 29 that illustrates how the stress is developed during heating and cooling, ending up as the residual stress. The intrinsic stress (open circles) is tensile and increases with increasing temperature basically due to film densification, but over the crystallization temperature, it decreases due to thermally activated atomic diffusion as well as to the manifested thermal stress.

(1) At low firing temperatures of 100–200 °C, the stress may be relaxed during cooling, but why it becomes compressive is left to be clarified.
(2) When the firing temperature is increased over 200 °C, the structural relaxation is less activated due to the progress of densification, which leads to an increase in tensile thermal stress ((ii) in Fig. 29). Such an increase in tensile thermal stress in conjunction with the increase in intrinsic stress provides the increase in residual tensile stress.
(3) The residual tensile stress slightly decreases at firing temperatures of 500–600 °C, which is attributed to the reduction in intrinsic stress due to thermally activated atomic diffusion as well as to manifested thermal stress ((iii) in Fig. 29).
(4) At firing temperatures over 600 °C, the tensile residual stress increases again, which results from the increase in tensile thermal stress generated during cooling ((iv) in Fig. 29). Such an increase in thermal stress results from the increase in Young's modulus of the film that is provided by the progress of crystallization and grain growth.

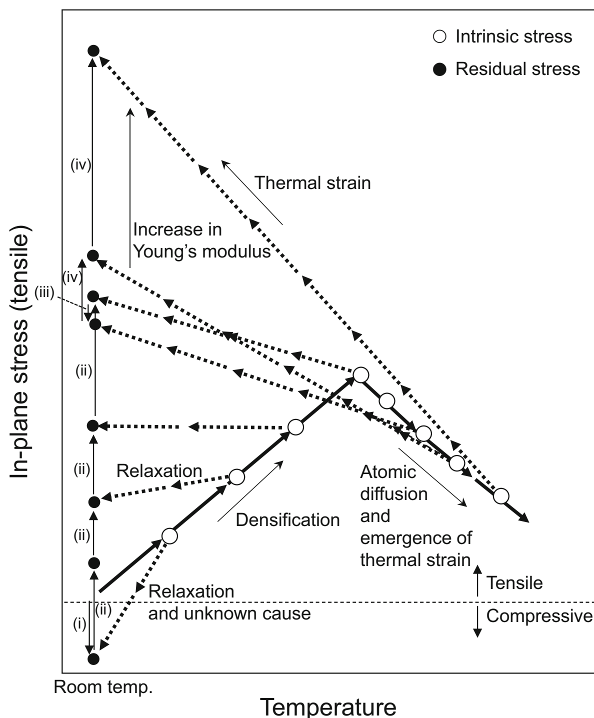

Fig. 29 Modified model showing how the stress develops in films during gel film-to-polycrystalline film conversion, illustrated on the basis of the present work. Intrinsic stress and residual stress are represented by open and closed circles, respectively. The model is drawn on the assumption that the fired films have larger thermal expansion coefficients than the substrate (Ohno et al. 2012)

Since the thermal stress generated during cooling constitutes a part of the residual stress, the trends illustrated in Fig. 29 should be very different when a different substrate is employed, while the intrinsic stress–temperature curve at temperatures below 500 °C may be identical in principle. Examination on the relationship between the residual stress and firing temperature is strongly desired for other combinations of films and substrates in order to understand fully the evolution of stress in sol-gel-derived oxide thin films.

Concluding Remarks

In spite of the great number of publication on gel-derived coatings, there is still lack of systematic and basic knowledge on sol-gel thin film formation, which is practically important for utilizing the sol-gel method for thin film production. Thinking in that way, experimental works have been done on stress evolution and cracking during gel film firing and on residual stress.

In situ measurement of stress in films demonstrated that in-plane tensile stress generated during gel film heating up is affected by water-to-alkoxide ratio, chelating agents, organic groups on alkoxides, and PVP. In situ observation of gel films under heating indicated that macroscopic cracking occurs in the heating-up stage and that

the cracking onset temperature is affected by heating rate, film thickness, water-to-alkoxide ratio, and humidity. The strategy for thick film formation without cracking via non-cycled deposition was reviewed, and PVP as plasticizer was demonstrated to be effective in increasing the uncracking critical thickness.

The in-plane residual stress was measured on YSZ films that were deposited on silicon substrates and fired at various temperatures. The dependence of the residual stress on the firing temperature was rather complex, but could be understood in terms of the increase in intrinsic stress during heating due to densification, the structural relaxation at low and high temperatures, and the thermal stress that is generated during cooling.

References

Al-Dahoudi N, Aegerter MA. Conducting, antistatic and antistatic-antiglare coatings made with hybrid sols. Mol Cryst Liq Cryst. 2002;374:91–100.
Al-Dahoudi N, Bisht H, Gobbert C, Krajewski T, Aegerter MA. Transparent conducting, anti-static and anti-static-anti-glare coatings on plastic substrates. Thin Solid Films. 2001;392:299–304.
Arscott S, Kurchania R, Miles RE, Milne SJ. Lead zirconate titanate thin films on GaAs substrates. J Mater Sci. 1997;32:6129–33.
Arscott S, Miles RE, Kennedy JD, Milne SJ. Rapid thermal processing of lead zirconate titanate thin films on Pt-GaAs substrates based on a novel 1,1,1-tris(hydroxymethyl)ethane sol-gel route. J Mater Res. 1999;14:494–9.
Atkinson A, Guppy RM. Mechanical stability of sol-gel films. J Mater Sci. 1991;26:3869–73.
Brenier R. Stress and moisture-sorption in ozone-annealed films of zirconium oxide obtained from sol-gel. J Sol-Gel Sci Techn. 2002;25:57–63.
Brenier R, Gagnaire A. Densification and aging of ZrO_2 films prepared by sol-gel. Thin Solid Films. 2001;392:142–8.
Brenier R, Urlacher C, Mugnier J, Brunel M. Stress development in amorphous zirconium oxide films prepared by sol-gel processing. Thin Solid Films. 1999;338:136–41.
Brinker CJ, Scherer GW. Sol-Gel Science. Boston: Academic; 1990.
Brinker CJ, Hurd AJ, Schunk PR, Frye GC, Ashley CS. Review on sol-gel thin film formation. J Non-Cryst Solids. 1992;147/148:424–36.
Cerqua KA, Hayden JE, LaCourse WCJ. Non-Cryst Solids. 1988;100:471–8.
Chewasatn S, Milne SJ. Sol-gel synthesis and electrical characterization of (Pb, Ca)TiO3 thin films. J Mater Sci. 1997;32:575–82.
Chiang CK, Wallace WE, Lynn GW, Feiler D, Xia W. Thermally induced stress relaxation and densification of spin-on-glass thin films. Appl Phys Lett. 2000;76:430–2.
Chingprado E, Reynesfigueroa A, Katiyar RS, Majumder SB, Agrawal DC. Raman-spectroscopy and X-ray-diffraction of $PbTiO_3$ thin-film. J Appl Phys. 1995;78:1920–5.
Chow LA, Dunn B, Tu KN, Chiang C. Mechanical properties of xerogel silica films derived from stress versus temperature and cracking experiments. J Appl Phys. 2000;87:7788–92.
Corkovic S, Whatmore RW, Zhang Q. Development of residual stress in sol-gel derived Pb(Zr, Ti) O3 films: An experimental study. J Appl Phys. 2008;103:084101.
Desu SB. Stress induced modifications in ferroelectric films. Phys Stat Sol (a). 1994;141:119–33.
Evans AG, Drory MD, Hu MS. The cracking and decohesion of thin films. J Mater Res. 1988;3:1043–9.
Exarhos GJ, Hess NJ. Spectroscopic measurements of stress-relaxation during thermally induced crystallization of amorphous titania films. Thin Solid Films. 1992;220:254–60.
Fujii M. Fundamental studies on crack formation in gel coatings during heat-treatment. Bachelor Thesis, Department of Materials Science and Engineering, Kansai University 2002 [in Japanese].

Garino TJ. The cracking of sol-gel films during drying. Mat Res Soc Symp Proc. 1990;180:497–502.

Gupta S. Investigations of micro-stress and phase transition in sol-gel-derived multideposited coatings of barium titanate using Raman spectroscopy. J Raman Spectr. 2002;33:42–9.

Hartner W, Bosk P, Schindler G, Bachhofer H, Mort M, Wendt H, Mikolajick T, Dehm C, Schroeder H, Waser R. $SrBi_2Ta_2O_9$ ferroelectric thin film capacitors: degradation in a hydrogen ambient. Appl Phys A Mater Sci Processing. 2003;77:571–9.

Hilgendorff M, Spanhel L, Rothenhausler C, Muller G. From ZnO colloids to nanocrystalline highly conductive films. J Electrochem Soc. 1998;145:3632–7.

Hoffman RW. The mechanical properties of thin condensed films. Phys Thin Films. 1966;3:211–73.

Hu MS, Thouless MD, Evans AG. The decohesion of thin films from brittle substrates. Acta Metall. 1988;36:1301–7.

Innocenzi P, Abdirashid MO, Guglielmi M. Structure and properties of sol-gel coatings from methyltriethoxysilane and tetraethoxysilane. J Sol-Gel Sci Techn. 1994;3:47–55.

Innocenzi P, Brusatin G, Guglielmi M, Signorini R, Meneghetti M, Bozio R, Maggini M, Scorrano G, Prato M. Optical limiting devices based on C-60 derivatives in sol-gel hybrid organic-inorganic materials. J Sol-Gel Sci Techn. 2000;19:263–6.

Ishikawa Y. In situ measurement of stress generated in titania and barium titanate gel films under heat-treatment: effects of chelating agents and polyvinylpyrrolidone on stress evolution. Master Thesis, Department of Materials Science and Engineering, Kanssai University 2004 [in Japanese].

Ishikawa Y, Kozuka H. Evolution of stress in alkoxide-derived titania gel films under heat-treatment: effects of polyvinylpyrrolidone and acetic acid in coating solutions. J Ceram Soc Jpn. 2004;112:S228–33.

Kozuka H. Issues on crack formation in sol-gel-derived ceramic coatings and thick film formation. Bull Ceram Soc Jpn. 2002;37:143–7 [in Japanese].

Kozuka H. On ceramic thin film formation from gels: evolution of stress, cracks and radiative striations. J Ceram Soc Jpn. 2003;111:624–32.

Kozuka H, Higuchi A. Single layer submicron thick $BaTiO_3$ coatings from PVP-containing sols: gel-to-ceramic film conversion, densification and dielectric properties. J Mater Res. 2001;16:3116–23.

Kozuka H, Higuchi A. Stabilization of PVP-containing alkoxide solutions for thick sol-gel $BaTiO_3$ films. J Am Ceram Soc. 2003;86:33–8.

Kozuka H, Kajimura M. Single-step dip-coating of crack-free $BaTiO_3$ films > 1 μm thick: Effect of poly(vinylpyrrolidone) on critical thickness. J Am Ceram Soc. 2000;83:1056–62.

Kozuka H., Kajimura M. Achievement of crack-free $BaTiO_3$ films over 1 μm in thickness via non-repetitive dip-coating. Chem Lett. 1999;28:1029–30.

Kozuka H, Komeda M. Effect of the amount of water for hydrolysis on cracking and stress evolution in alkoxide-derived sol-gel silica coating films. J Ceram Soc Jpn. 2004;112:S223–7.

Kozuka H, Takenaka S. Single-step deposition of gel-derived PZT films: critical thickness and gel-to-ceramic film conversion. J Am Ceram Soc. 2002;85:2696–702.

Kozuka H, Kajimura M, Hirano T, Katayama K. Crack-free, thick ceramic coating films via non-repetitive dip-coating using polyvinylpyrrolidone as stress-relaxing agent. J Sol-Gel Sci Techn. 2000;19:205–9.

Kozuka H, Isota Y, Higuchi A, Hamatani T. Cracks in gel-derived ceramic coatings and thick film formation. In: Miyata N, Ota R, Miyamoto Y, Shiono T, editors. Proceedings of international symposia on materials science for the 21th century, vol. B. Kyoto: The Society of Materials Science; 2001a. p. 122–5.

Kozuka H, Isota Y, Hosokawa M. Ceramic processing science VI. In: Hirano, S, Messing, GL, Claussen N, editors. Ceram. Trans, vol. 112. Westerville: American Ceramic Society; 2001b. p. 335–40.

Kozuka H., Katayama K., Isota Y., Takenaka S. Achievement of crack-free ceramic coatings over 1 μm in thickness via single-step deposition. In: Feng X, Klein LC, Pope EJA, Komarneni S, editors. Sol-Gel commercialization and applications. Westerville: American Ceramic Society; 2001c. p. 105–10.

Kozuka H, Takenaka S, Tokita H, Hirano T, Higashi Y, Hamatani TJ. Sol-Gel Sci Techn. 2003;26:681–6.

Kozuka H, Takenaka S, Tokita H, Okubayashi M. PVP-assisted sol-gel deposition of single layer ferroelectric thin films over submicron or micron in thickness. J Eur Ceram Soc. 2004;24:1585–8.

Lee JH, Choo WK, Kim YS, Yun DW. Depth-dependent lattice-parameter variation and stress-induced magnetic-anisotropy of ultrathin $Dy_2BiFe_4GaO_{12}$ garnet-films deposited on the glass substrate by pyrolysis. J Appl Phys. 1994;75:2455–9.

Lian L, Sottos NR. Stress effects in sol-gel derived ferroelectric thin films. J Appl Phys. 2004;95:629–34.

Lu J, Kobayashi T, Zhang Y, Maeda R, Mihara T. Wafer scale lead zirconate titanate film preparation by sol-gel method using stress balance layer. Thin Solid Films. 2006;515:1506–10.

Maki K, Soyama N, Nagamine K, Mori S, Ogi K. Low-temperature sintering of ferroelectric Pb(Zr, Ti)O3 thick films derived from stable sol-gel solutions. Integr Ferroelectrics. 2001;41:1819–26.

Mehner A, Klumper-Westkamp H, Hoffmann F, Mayr P. Crystallization and residual stress formation of sol-gel-derived zirconia films. Thin Solid Films. 1997;308:363–8.

Mendiola J, Calzada ML, Ramos P, Martin MJ, Agullo-Rueda F. On the effects of stresses in ferroelectric (Pb, Ca)TiO3 thin films. Thin Solid Films. 1998;315:195–201.

Miyake H. Effects of trialkoxysilane and polyvinylpyrrolidone on the uncracking critical thickness and stress of sol-gel-derived silica thin films. Bachelor Thesis, Department of Materials Science and Engineering, Kanssai University 2003 [in Japanese].

Nakai N, Kozuka H. PVP-assisted sol-gel preparation of $BaBi_4Ti_4O_{15}$ thin films and dielectric properties. Trans Mater Res Soc Jpn. 2004;29:2269–72.

Ohno T, Matsuda T, Ishikawa K, Suzuki H. Thickness dependence of residual stress in alkoxide-derived $Pb(Zr_{0.3}Ti_{0.7})O_3$ thin film by chemical solution deposition. Jpn J Appl Phys Pt 1. 2006;45:7265–9.

Ohno T, Malic B, Fukazawa H, Wakiya N, Suzuki H, Matsuda T, Kosec M. Origin of compressive residual stress in alkoxide derived $PbTiO_3$ thin film on Si wafer. Jpn J Appl Phys Pt 2. 2008;47:7514–8.

Ohno K, Uchiyama H, Kozuka H. Understanding of the development of in-plane residual stress in sol-gel-derived metal oxide thin films. J Appl Phys. 2012;111:014901.

Ohya Y, Itoda S, Ban T, Takahashi Y. Lead zirconate titanate thick films fabricated from sols with and without its powder. Jpn J Appl Phys Pt 1. 2002;41:270–4.

Parrill TM. Heat-treatment of spun-on acid-catalyzed sol-gel silica films. J Mater Res. 1994;9:723–30.

Pulskamp JS, Wickenden A, Polcawich R, Piekarski B, Dubey M, Smith G. Mitigation of residual film stress deformation in multilayer microelectromechanical systems cantilever devices. J Vac Sci Techn B. 2003;21:2482–6.

Robertson MA, Rudkin RA, Parsonage D, Atkinson A. Mechanical and thermal properties of organic/inorganic hybrid coatings. J Sol-Gel Sci Techn. 2003;26:291–5.

Rossetti Jr GA, Cross LE, Kushida K. Stress induced shift of the Curie point in epitaxial $PbTiO_3$ thin films. Appl Phys Lett. 1991;59:2524–6.

Saegusa T, Chujo Y. An organic/inorganic hybrid polymer. J Macromole Sci Chem. 1990; A27:1603–12.

Saegusa T, Chujo Y. Organic-inorganic polymer hybrids. Makromol. Chem, Macromol Symp. 1992;64:1–9.

Scherer GW. Recent progress in drying of gels. J Non-Cryst Solids. 1992;147/148:363–74.

Sendova M, Willis K. Spiral and curved periodic crack patterns in sol-gel films. Appl Phys A Mater Sci Proc. 2003;76:957–9.

Sengupta SS, Park SM, Payne DA, Allen LH. Origins and evolution of stress development in sol-gel derived thin layers and multideposited coatings of lead titanate. J Appl Phys. 1998;83:2291–6.

Sriprang N, Kaewchinda D, Kennedy JD, Milne SJ. Processing and sol chemistry of a triol-based sol-gel route for preparing lead zirconate titanate thin films. J Am Ceram Soc. 2000;83:1914–20.

Syms RRA. Stress in thick sol-gel phosphosilicate glass films formed on Si substrates. J Non-Cryst Solids. 1994;167:16–20.
Syms RRA, Holmes AS. Deposition of thick silica titania sol-gel films on Si substrates. J Non-Cryst Solids. 1994;170:223–33.
Takenaka S, Kozuka H. Sol-gel preparation of single-layer, 0.75 μm thick lead zirconate titanate films from lead nitrate-titanium and zirconium alkoxide solutions containing polyvinylpyrrolidone. Appl Phys Lett. 2001;79:3485–7.
Thouless MD. Decohesion of films with axisymmetric geometries. Acta Metall. 1988;36:3131–5.
Tu YL, Milne SJ. A study of the effects of process variables on the properties of PZT films produced by a single-layer sol-gel technique. J Mater Sci. 1995a;30:2507–16.
Tu YL, Milne SJ. Characterization of single-layer PZT (53/47) films prepared from an air-stable sol-gel route. J Mater Res. 1995b;10:3222–31.
Tu YL, Calzada ML, Phillips NJ, Milne SJ. Synthesis and electrical characterization of thin films of PT and PZT made from a diol-based sol-gel route. J Am Ceram Soc. 1996;79:441–8.
Tuchiya T, Itoh T, Sasaki G, Suga T. Preparation and properties of piezoelectric lead zirconate titanate thin films for microsensors and microactuators by sol-gel processing. J Ceram Soc Jpn. 1996;104:159–63.
Wu W, Lanagan MT, Kullberg ML, Poeppel RB, Wang B, Danyluk S. The relationship between microstructure and residual-stress in $YBa_2Cu_3O_{7-x}$. Thin Solid Films. 1993;223:260–8.
Yao K, Yu SH, Tay FEH. Residual stress analysis in ferroelectric $Pb(Zr_{0.52}Ti_{0.48})O_3$ thin films fabricated by a sol-gel process. Appl Phys Lett. 2003;82:4540–2.
Zhang LL, Ichiki M, Maeda R. Stress measurements of Pt/PZT/Pt thin-film stack on oxidized silicon substrate for micro-actuator. Ferroelectrics. 2002;273:2461–6.
Zhang LL, Ichiki M, Maeda R. Residual stresses in Pt bottom electrodes for sol-gel derived lead zirconate titanate thin films. J Eur Ceram Soc. 2004;24:1673–6.